478 | Dezember 1986

SCHRIFTENREIHE SCHIFFBAU

Lajpat Rai Raheja

Free Surface Shear Flow Model for Bow Vortices Phenomena

TUHH
Technische Universität Hamburg-Harburg

Free Surface Shear Flow Model for Bow Vortices Phenomena

Lajpat Rai Raheja, Hamburg, Technische Universität Hamburg-Harburg, 1986

Schriftenreihe Schiffbau
Schwarzenbergstraße 95c
D-21073 Hamburg

http://www.tuhh.de/vss

INSTITUT FÜR SCHIFFBAU DER UNIVERSITÄT HAMBURG

Bericht Nr. 478

Free Surface Shear Flow Model for Bow Vortices Phenomena

by

Lajpat Rai Raheja

Dezember 1986

ISBN 3 - 89220 - 478 - 0

 Institut für Schiffbau
Universität Hamburg
Lämmersieth 90
D-2000 Hamburg 60

ACKNOWLEDGEMENT

The author is grateful to Prof. K. Eggers, under whose supervision the project has been carried out, for his valuable suggestions and constant encouragement. Thanks are also due to Prof. S.D. Sharma for helpful discussions.

The author wishes to express his cordial thanks to Prof. H. Keil, Director, and the faculty and staff of the IFS for their warm hospitality.

Last but not the least, the financial support from the Deutsche Forschungsgemeinschaft under Contract No. Eg 26/11-1 is gratefully acknowledged.

ABSTRACT

Experiments by Sharma, Eggers and others in the Institut fur Schiffbau, Hamburg showed that when a horizontal circular cylinder is towed semisubmerged at a uniform speed, there exists a free surface shear layer ahead of the cylinder. The deceleration of the fluid particles in the free surface boundary layer gives rise to vortices before the body and a free surface separation point which separates the vortex zone near the body from rest of the flow. These observations provided an explanation to the origin of the phenomenon of bow-wave-breaking which occurs as vortical motion ahead of the ships with usually blunt bows and extends all around the hull commonly called as necklace vortex.

In the present study an attempt is made to formulate a shear flow-model for the free surface flow ahead of the cylinder in the framework of boundary layer theory in order to provide a theoretical analysis to the experimental observations. The vorticity generated due to viscous forces at the boundary is assumed to be concentrated in a thin free surface boundary layer while the flow underneath this layer is assumed to be potential. Karman-Pohlhausen method is used to solve the two dimensional boundary layer equations in curvilinear coordinates. The boundary layer profile is assumed to be a cubic satisfying stress and velocity conditions at the boundary. The velocity defect in the boundary layer is assumed to be relatively small in order to simplify the problem. The free surface configuration which needed to be prescribed for the computations is substituted from that of constant pressure surface of the double body flow without satisfying any kinematic condition.

The computations show that the free surface flow slows down relative to the potential flow and the velocity defect increases as the distance from the cylinder decreases. The free surface velocity becomes negative resulting in back-flow ahead of the cylinder as observed in the experiment. This however occurs at exceedingly close distances from the cylinder. The computation of the boundary layer profile shows a regular growth of shear as the body is approached. The free surface separation point moves away from the cylinder as the Froude number is increased which is also in agreement with the experimental observations. The occurrence of the free surface separation point at exceedingly close distances from the body which is against the experimental observations stresses the need for an improvement in the analysis.

An attempt was made to obtain free surface and the potential flow velocity components incorporating surface

tension and viscosity. It did not result in a better separation criterion. The reason for that was found in the fact that the analysis assumed a uniform basic flow instead of a flow with gradient which is essential for the growth of free surface shear layer.

It is apprehended that the presence of a point of inflexion in the boundary layer profile results in instability and back flow before the free surface velocity becomes negative and gives vortices. That the present analysis shows the separation to occur exceedingly close to the body contrary to experimental observation may be possibly explained by the fact that instability has not been considered. However, a stability analysis would be necessary to confirm this point.

Zusammenfassung

Der Auslöser für diese Untersuchung waren im Institut vorausgegangene Schleppversuche mit teilgetauchten Kreiszylindern, bei denen Bugwirbel vor dem Schleppkörper unmittelbar unter der freien Wasseroberfläche beobachtet wurden. In dieser Arbeit wurde versucht, eine theoretische Erklärung für dieses Phänomen zu finden. Dazu wurde die ebene Strömung unter der freien Wasseroberfläche vor einem quer zu seiner Achse halbgetaucht geschleppten horizontalen Kreiszylinder mit Hilfe eines Grenzschichtansatzes berechnet. Die durch viskose Kräfte an der (leicht) gekrümmten freien Wasseroberfläche erzeugte Vortizität verbleibt in einer dünnen Grenzschicht, während darunter im wesentlichen Potentialströmung herrscht. Die Berechnungen ergaben, daß die Strömung auf der freien Oberfläche (im mitbewegten Koordinatensystem) mit Annäherung an den Zylinder allmählich abgebremst wird, bis sich schließlich das Vorzeichen umkehrt und eine Sekundärströmung in der Gestalt eines Bugwirbels entsteht, während die Primärströmung unter dem Zylinder hindurchfließt. Der berechnete Ablösepunkt der Grenzschicht an der freien Oberfläche wandert zwar mit zunehmender Froudezahl nach vorn, liegt jedoch im Vergleich zum Experiment viel zu nahe vor dem Zylinder. Möglicherweise sind Stabilitätsbetrachtungen erforderlich, um das theoretische Strömungsmodell zu verbessern.

CONTENTS

1. INTRODUCTION

It is usual to observe a foaming motion at the bow of a full ship extending all around the hull distinctly in addition to the wave pattern emerging from the proximity of the hull joining this motion. This vortical motion is known as bow vortices or bow wave breaking as the wave profile looks having broken at the bow and given rise to bow vortices. The vortices also extend all round the hull forming a chain commonly called necklace vortex. The phenomena is more pronounced with fuller ship forms and high Froude numbers.

It was recognised by Baba (1969) and by Eckert and Sharma (1970) that bow vortices are responsible for a significant part of a ship's total resistance particularly in case of full form ships. Owing to the highly nonlinear nature of the phenomena the linear theories of wave resistance fail to account for its contribution. This is also thought to be one of the reasons for the poor performance of wave resistance theories as compared to the much cruder theories of seakeeping.

The investigations conducted on this phenomena, experimental as well as theoretical, can be classified into two groups, (a) those conducted with the aim of reducing the bow wave breaking, which may be termed as design improvement oriented investigations, (b) those

conducted with the sole aim of understanding the hydrodynamic mechanism of bow wave breaking, which may be termed as theory improvement oriented investigations. The latter group can further be divided into two subgroups according to the underlying concept of investigations, namely, (i) Shock wave concept oriented investigations and (ii) Shear layer concept oriented investigations. The present investigation analyses the free surface shear layer in relation to the bow vortices phenomena and consequently falls in the latter subgroup. However we shall briefly review the existing research work on the phenomena in the order of the classification mentioned above before describing the present investigation in detail.

(A) Design improvement oriented investigations

The early pioneering work of Baba (1969), Eckert and Sharma (1970), Taneda (1969) and Taiguchi et al. (1972) examined the effects of ship form parameters and various shapes of bow protruding bulbs on bow wave breaking using wake survey method and resistance tests. Takekuma and Eggers (1984) using flow visualisation and image processing techniques showed that bow forms with fine entrance angles and the protruding bulbs are effective in reducing bow vortices. Mori (1984) in his experiments on velocity measurement in bow flow found that bow bulb gives a slight change in the wave profile but yields a big change in the

velocity field consisting of mainly decrease in turbulent intensities and Reynolds stresses. Ogiwara (1984) used a bow wing as a measure to reduce the ship resistance and found that it is effective in reducing the free surface turbulence at the bow thereby reducing bow wave breaking. On the theoretical side, the existence of smooth continuous solutions having neither splashes nor waves was examined by Tuck and Vanden-Broeck (1984). They demonstrated numerically the existence of such body shapes with the corresponding solutions modelling the bow flows in which the splash drag component is completely eliminated. The bow shapes for which this elimination is possible were found to be only bulbous.

(B) Theory improvement oriented investigations

(i) Shock wave concept oriented

Miyata and Inui (1984) conducted detailed measurements of the velocity field in the vicinity of the free surface around ship models. The authors prefer to call the nonlinear ship waves as Free Surface Shock waves because of some of its typical characteristics which they summarise as follows: (1) steepness of the wave slope, (2) formation of lines of discontinuity, (3) turbulence on the free surface on and behind the wave front, (4) systematic changes of the wave-crest-line-angle,

depending upon the Froude number and the ship model configuration, (5) satisfaction of a kind of shock relation across the wave fronts, and (6) dissipation of wave energy into momentum loss far behind the ship model.

Miyata et al. (1983, 1984a,b, 1985a) have used a modified version of the Marker and Cell (MAC) method called by them as TUMAC method (TU perhaps stands for Tokyo University) to simulate numerically the bow wave breaking phenomenon on a two dimensional rectangular body. No slip condition has been satisfied. It is claimed that supporting evidence on their conjecture about the characteristics of free surface shock waves has been obtained. According to the computation, the first wave in front of the bow steepens and overturns and consequently this overturning motion generates a rotational motion with significant intensity at the wave front. With the forward advance of the wave front with spilling breakers the layer of vortical motion extends beneath the free surface, and this region of vorticity reaches the forward wall of the body.

The numerical simulation of three dimensional bow waves using the TUMAC method has been reported by Miyata and Inui (1984). For a more detailed review on numerical simulation of bow waves the reader is referred to the 18th ITTC - Resistance and Flow Committee Report.

(ii) Shear flow concept oriented

Takekuma (1972) conducted a series of flow measurements around the bow of a full ship model using a five hole pitot tube with the aim to provide material for a rational mathematical model for the bow vortices phenomenon. The results of velocity component measurements were compared with those obtained from the potential flow theory using double body flow. Except for the thin layer below the free surface, the velocity components agreed well. In this thin layer, the velocity components changed abruptly in vertical direction. These observations suggested the importance of a detailed study of the conspicuous behaviour of the flow in the thin layer below the free surface which later came to be known as free surface shear layer. Honji (1976) conducted experiments on flow past semisubmerged cylinders, found that there is a region of vortices ahead of the cylinder separated by a sharp boundary from the basic orderly flow on the free surface. Further, this free surface separation point (FSSP) moves away from the cylinder with increase in Froude number, Fig. (1)-(2). Kayo and Takekuma (1981),(1983) visualised the flow ahead of full ship models using metal flakes and water colour dye. The authors concluded the existence of a shear layer just below the free surface. It turned out further that the intensity of the shear

layer was related to the intensity of vortices before the body. This was confirmed by artificially increasing the intensity of the shear layer by towing a polyvinyl sheet ahead of the body. Later, in a second series of experiments on semisubmerged circular cylinders and ship models respectively by Kayo, Takekuma, Eggers and Sharma (1982) and Kayo and Takekuma (1983), the shear layer and bow vortices were visualised by water colour dye and the position of the free surface separation point was measured for different Froude numbers, Fig. (3).

The variation of FSSP with Froude number for a horizontal circular cylinder is not monotonically increasing (Fig. 3) but shows an interesting behaviour. Sharma (private discussion) interpreted that this behaviour over the range of Froude numbers could be divided into three parts according to the nature of variation. From zero to app $F = 0.23$, the position of FSSP is quite far from the cylinder and also is somewhat unpredictable. This could be explained by the surface rigidity phenomenon where the free surface behaves like a stationary film with some rigidity due to contamination particles and a boundary layer can develop beneath it, Harper and Dixon (1974). At the leading edge of such a film, a sharp ridge called Reynolds ridge is formed. Scott (1982) measured the slope of this ridge and compared it with the slope provided by Harper and Dixon's theory.

The unpredictability in this region is due to uncertain contamination levels at each run. The boundary of this region (F = .23) corresponds to a speed of app. 0.23 m/sec, which is the threshold speed for capillary waves to be important, as below this speed gravity waves will not be formed. By and large surface tension dominates in this zone. For the second region, i.e. F = .23 to F = .5 app., the curve shows a monotonic increase in the distance of FSSP from the body. The vortices increase with speed, but still the speed is small enough not to create turbulence or surface breaking. For speeds higher than this, i.e. in third region, the trend is not a definite one. This may be assigned to the fact that now the free surface starts breaking and vortices are replaced with a turbulent motion. In three dimensional flows, bow vortices were observed by Shahshahan (1981) on ship models, by Kayo Takekuma, Sharma and Eggers (1982) on vertical cylinders.

Some further attempts were made to understand the bow vortices phenomenon by photographing the free surface ahead of the body using metal flakes and analysing its configuration, Mori (1984), Maruo (1986), Miyata and Inui (1984). Authors also introduced the concept of sub-breaking waves which appear prior to breaking waves.

Along with the above described experimental and numerical studies, there were attempts for a theoretical model of bow flow and bow vortices. Dagan and Tulin (1972, 1974) treated the problem of bow flow as a free surface

gravity flow and the breaking of the surface was assigned to Taylor instability associated with the curvature of the stream lines and speed of flow. This method is based upon two perturbation expansions using Froude number as parameter. A critical value of Froude number is found for instability.*) Shahshahan (1981) considered two kinds of instabilities, one due to longitudinal curvature of streamlines and other due to lateral curvature of streamlines near the stagnation region. Following a suggestion of Baba (1981) that there might be an analogy between the necklace vortex and a horseshoe vortex of a vertical strut piercing a flat plate, Takekuma and Eggers (1984) applied the theory of secondary flow by Hawthorne (1954) to evaluate the dependence of secondary vorticity components on some major ship form parameters. Their idea was, besides understanding the hydrodynamic mechanism of bow vortices, to obtain useful hints on bow shapes to help the design of full form ships. The analysis showed that no stationary free surface shear flow can exist where the free surface does not display curvature. Mori (1984) calculated the vorticity distribution in the potential flow past a circular cylinder with constant upstream vorticity according to Lighthill's (1956) drift theory. The result showed a marked accumulation of vorticity at the bow and a rapid development of its longitudinal component around the cylinder similar to the occurence of bow vortices and the necklace vortex.

*) The occurrence of Taylor instability over a certain Froude number was supported experimentally by Suzuki (1975).

Patel et al. (1985) treated the two dimensional free surface shear layer as a boundary layer across which vorticity takes a jump. This layer of vorticity has potential flow below it and a non zero value of vorticity at the free surface is arising out of the requirement for a vanishing tangential stress on the curved free surface. The authors further assume a selective balance of forces in the normal stress boundary condition on the free surface, namely pressure jump across the free surface is zero and the surface tension force is balanced by the normal viscous force, instead of the exact boundary condition in which the pressure jump is balanced by surface tension and normal viscous force. The authors derive a simple separation criterion (Fig. 2-3) based upon the latter part of the assumption only from kinematics without resorting to solving the momentum equations. The criterion involves Reynolds and Weber numbers along with the slope of the free surface which brings Froude number into it. A free surface is then obtained using the zero pressure jump condition in potential flow and satisfying additionally a kinematic condition. Substituting the velocity components of a double body flow, the slope of the free surface is evaluated as a function of Froude number and subsequently the separation criterion. The values of free surface separation point (FSSP) so obtained agree approximately

with the experimental values of Kayo, Takekuma, Eggers and Sharma (1982) for a certain range of Froude number. This according to them explains the origin of bow vortices. The authors further analysed the Navier-Stokes equations and formulated the boundary layer problem using the Karman-Pohlhausen method, but the equations were left unintegrated.

The review of the work done on the bow vortices problem as presented above shows that though the free surface shear layer is clearly visualised and its relation with bow vortices problem is established but to the best of our knowledge, a theoretical model of free surface shear layer resulting into bow vortices is not yet available. In the present investigation, an attempt is made to formulate a shear layer model of the free surface flow ahead of a body. A horizontal semisubmerged circular cylinder is assumed to be moving with a uniform speed. The two dimensional free surface shear layer is analysed as a boundary layer of vorticity adjoining the potential flow. The origin of vorticity lies in the viscous forces acting on the free surface. A simplifying assumption is made, namely velocity defect in the shear layer is small as compared to potential flow (Batchelor 1970). The equations are integrated and the velocity profile in the free surface shear layer is computed at various positions ahead of the body. The profile shows a regular increase in shear as it

moves nearer to the body. A close form separation criterion is not found to be possible. However, the computation of free surface velocity shows that the free surface moves slower than the corresponding potential flow beneath it and a reversal of velocity which occurs, though exceedingly close to the body, confirms the separation. The onward sections of the report give in detail the formulation of the problem, its solution and discussion of results. An improvement of the model using wave theory with surface tension and viscous effects is also attempted. Report ends with a section on conclusions.

2. FORMULATION OF THE PROBLEM

Consider a horizontal semisubmerged circular cylinder in a uniform stream with velocity U_∞. The obstacle will give rise to a two dimensional curved free surface rising above the undisturbed level. Along with a Cartesian system of coordinates (Fig. 3), it will be convenient to work with a curvilinear coordinate system (S,n) where S is the coordinate along the stream line and n is the coordinate normal to it. Let u and v be the corresponding velocity components and ζ the elevation of the free surface above the undisturbed level.

The flow will be governed by the equation of continuity and the Navier-Stokes equations, which written in curvilinear coordinates are (Patel 1985),

$$\frac{1}{h_1}\frac{\partial u}{\partial s} + \frac{\partial v}{\partial n} + k_{12} v = 0 \qquad (2.1)$$

$$\frac{u}{h_1}\frac{\partial u}{\partial s} + v\frac{\partial u}{\partial n} + k_{12} u v + \frac{1}{h_1}\frac{\partial}{\partial s}(p/\rho) + \frac{g}{h_1}\frac{\partial y}{\partial s} = \nu\left[\frac{1}{h_1^2}\frac{\partial^2 u}{\partial s^2}\right.$$

$$\left. + \frac{\partial^2 u}{\partial n^2} - \frac{1}{h_1^3}\frac{\partial h_1}{\partial s}\frac{\partial u}{\partial s} + k_{12}\frac{\partial u}{\partial n} + 2k_{12}\frac{1}{h_1}\frac{\partial v}{\partial s} - k_{12}^2 u + \frac{1}{h_1}\frac{\partial k_{12}}{\partial s} . v\right] \qquad (2.2)$$

$$\frac{u}{h_1}\frac{\partial v}{\partial s} + v\frac{\partial v}{\partial n} - k_{12} u^2 + \frac{\partial}{\partial n}(p/\rho) + g\frac{\partial y}{\partial n} = \nu\left[\frac{1}{h_1^2}\frac{\partial^2 v}{\partial s^2} + \frac{\partial^2 v}{\partial n^2}\right.$$

$$\left. - \frac{1}{h_1^3}\frac{\partial h_1}{\partial s}\frac{\partial v}{\partial s} + k_{12}\frac{\partial v}{\partial n} - 2k_{12}\frac{1}{h_1}\frac{\partial u}{\partial s} - \frac{1}{h_1}\frac{\partial k_{12}}{\partial s} . u - k_{12}^2 v\right] \qquad (2.3)$$

where ρ, g, ν, p are respectively density, acceleration due to gravity, kinematic viscosity and fluid pressure. Further,

$$h_1 = 1 + kn$$

$$k_{12} = \frac{1}{h_1}\frac{\partial h_1}{\partial n} = \frac{k}{1+kn} \qquad (2.4)$$

Here k is the curvature of the free surface.

The solution of above equations must satisfy the following boundary conditions:

- no slip at the body
- tangential stress equal to zero at the free surface

- total normal stress equal to zero at the free surface, which in other words means that the pressure jump should be balanced by surface tension and normal viscous stress.

It is well understood that such a solution is extremely difficult to find. However, we shall consider some simplifications.

2.1 Free surface shear layer

It is well known that a potential flow solution is also a solution of the Navier-Stokes equations, but it fails to satisfy the viscous boundary conditions. We shall examine such a solution with respect to the second boundary condition, i.e. requirement of vanishing tangential stress at the free surface. Let us first assume that the free surface is flat. Since the flow is irrotational, vorticity is equal to zero. The only component of vorticity

$$\omega = \frac{\partial v}{\partial x} - \frac{\partial u}{\partial y} = 0 \text{ , or } \frac{\partial v}{\partial x} = \frac{\partial u}{\partial y} \text{ everywhere} \qquad (2.5)$$

Since the normal velocity $v = 0$ at each point of the free surface so $\frac{\partial v}{\partial x} = 0$ at the free surface and consequently $\partial u / \partial y = 0$. The requirement of vanishing tangential stress demands

$$\tau_{xy} = \mu \left[\frac{\partial u}{\partial y} + \frac{\partial v}{\partial x} \right] = 0$$

at the free surface, where μ is the coefficient of viscosity. Since $\partial u/\partial y$ and $\partial v/\partial x = 0$ at the free surface as shown above, the requirement is thus satisfied.

Now, we examine the same solution when the free surface is not flat but curved.

$$\text{Vorticity} = \omega = \frac{1}{h_1} \left\{ \frac{\partial v}{\partial s} - \frac{\partial}{\partial n}(h_1 u) \right\} = 0 \qquad (2.6)$$

This gives

$$\frac{\partial v}{\partial s} = \frac{\partial (h_1 u)}{\partial n} \qquad \text{everywhere,}$$

where $h_1 = 1 + kn$, k being the curvature of the free surface. Since $v = 0$ at each point of the free surface, therefore $\partial v/\partial s = 0$ at the free surface. The condition (2.6) gives, at the free surface

$$\left(\frac{\partial u}{\partial n} \right)_0 = -k u_0 \qquad (2.7)$$

where subscript 0 stands for the free surface,

The tangential stress at the free surface is given as

$$\tau_{sn_0} = \mu \left[h_1 \frac{\partial}{\partial n} \left(\frac{u}{h_1} \right) + \frac{1}{h_1} \frac{\partial v}{\partial s} \right]_0$$

Since $\frac{\partial u}{\partial s} = 0$ at the free surface, we obtain

$$\tau_{sno} = \mu\left[\frac{\partial u}{\partial n} - k u\right]_o \qquad (2.8)$$

From equations (2.7) and (2.8), we get

$$\tau_{sno} = -2\mu k u_o \qquad (2.9)$$

Hence, the requirement for vanishing tangential stress is not satisfied at a curved free surface.

A non-zero value of tangential stress close to the boundary accelerates the fluid particles along the boundary so as to reduce the stress to zero. This acceleration (retardation in this case as the τ_{sno} is negative) of the fluid by viscous forces generates vorticity which then diffuses into the fluid in a familiar manner. The vorticity so generated can be straightway obtained by setting τ_{sno} equal to zero, which then gives

$$\frac{\partial u}{\partial n} = k u_o$$

Eliminating $\partial u/\partial n$ from equation (2.6) using the above relation, we obtain

$$\omega_o = -2 k u_o$$

A simplification can now be introduced by assuming that the vorticity in the flow is concentrated in a thin layer below the free surface while the rest of the flow is irrotational. This thin layer across which vorticity changes its value from zero (in potential flow) to $-2kU_0$ at the free surface is a free surface boundary layer or free surface shear layer. It may be noted that viscous forces give rise to this layer only in the presence of curvature. This free surface shear layer is observed in the experiments and is responsible for bow vortices generation. We shall now aim to calculate the velocity profile in this layer.

Equations of motion (2.1 - 2.3) can now be simplified by making an order of magnitude analysis (Patel 1985) as done in the case of the usual Prandtl's boundary layer equations. Let L and δ be respectively the characteristic length and the boundary layer (free surface shear layer) thickness. The nondimensional free surface curvature which depends upon body geometry and the other parameters may be written as $k^* = kL$. Taking

$$u = O(U_\infty) \quad , v = O\left(\frac{\delta}{L} U_\infty\right) \tag{2.9}$$

we have from the equation of continuity

$$\frac{\partial u}{\partial s} + h_1 \frac{\partial v}{\partial n} + k v = 0 \tag{2.10}$$

$$\frac{\partial u}{\partial s} = \frac{\partial v}{\partial n} = O\left(\frac{U_\infty}{L}\right) \tag{2.11}$$

From equation (2.7), we have

$$\frac{\partial u}{\partial n} = O\left(k^* \frac{U_\infty}{L}\right) \tag{2.12}$$

which further gives

$$\frac{\partial^2 u}{\partial n^2} = O\left(k^* \frac{L}{\delta}\right) \frac{U_\infty}{L^2} \tag{2.13}$$

Differentiating equation (2.10) with respect to we get

$$\frac{\partial^2 u}{\partial s \partial n} + h_1 \frac{\partial^2 v}{\partial n^2} + 2k \frac{\partial v}{\partial n} = 0 \tag{2.14}$$

Substituting the results from equations (2.11) and (2.12), we get

$$\frac{\partial^2 v}{\partial n^2} = O(k^*) \frac{U_\infty}{L^2} \tag{2.15}$$

Now, since the first convective term together with the pressure and gravity in the momentum equation (2.2) yields

the Bernoulli equation, we conclude that the leading viscous term must be of the order $O(k\delta)$ i.e.

$$\nu \frac{\partial^2 u}{\partial n^2} = \frac{k^* L}{Re\,\delta} \cdot \frac{U_\infty^2}{L} = O(k\delta) \frac{U_\infty^2}{L}$$

Hence

$$\frac{\delta}{L} = O \frac{1}{\sqrt{Re}} \tag{2.16}$$

and further the equations (2.9) and (2.13) can be written as

$$v = O\left(\frac{1}{\sqrt{Re}}\right) U_\infty \tag{2.17}$$

$$\frac{\partial^2 u}{\partial n^2} = O\left(k^* \sqrt{Re}\right) \frac{U_\infty}{L^2} \tag{2.18}$$

Summarising the results we have

$$u = O(1)\, U_\infty, \quad v = O\left(\frac{1}{\sqrt{Re}}\right) U_\infty$$

$$\frac{\partial u}{\partial n} = O(k^*) \frac{U_\infty}{L}, \quad \frac{\partial v}{\partial n} = O(1) \frac{U_\infty}{L} \tag{2.19}$$

$$\frac{\partial^2 u}{\partial n^2} = O\left(k^* \sqrt{Re}\right) \frac{U_\infty}{L^2}, \quad \frac{\partial^2 v}{\partial n^2} = O(k^*) \frac{U_\infty}{L^2}$$

When these orders of magnitudes are introduced into the equations (2.1) - (2.3) and the terms upto the order $O(k\delta)$

are retained in each equation, we obtain the following boundary layer equations:

$$\frac{\partial u}{\partial s} + \frac{\partial v}{\partial n} = 0 \qquad (2.20)$$

$$u\frac{\partial u}{\partial s} + v\frac{\partial u}{\partial n} + kuv = -\frac{\partial}{\partial s}(p/\rho + gy) + \nu\frac{\partial^2 u}{\partial n^2} \qquad (2.21)$$

$$ku^2 = \frac{\partial}{\partial n}(p/\rho + gy) \qquad (2.22)$$

2.2 Linearisation

The free surface boundary layer thus formed is such that the vorticity across this layer makes a jump from its zero value in the adjoining potential flow to the value $-2ku_0$ at the free surface. Thus the jump in vorticity across this layer is

$$\Delta\omega = 2ku_0$$

The jump in velocity across the layer evidently is of the order of $\delta . \Delta\omega$ being the boundary layer thickness. Hence the variation of velocity in the boundary layer is small. This means that the velocity in the boundary layer

is not very much different from the corresponding velocity in the potential flow. This smallness of variation has three noteworthy implications (Batchelor 1970): (a) the equations of motion for the boundary layer can be linearised with respect to departure of velocity from the value just outside the boundary layer; (b) the tendency of backflow to develop in the boundary layer at a free surface is very much weaker as compared to that at a rigid boundary in the usual boundary layer, and separation is unlikely to occur unless there is a large curvature of the boundary; (c) since the velocity gradients within the boundary layer are not of a larger order of magnitude than outside it, the rate of dissipation per unit volume is of the same order throughout the fluid. Thus the total rate of dissipation is dominated by the contribution from the more extensive region of potential flow, in contrast with the case of flow with the boundary layer at a rigid wall, for which the contribution to the total dissipation from the region of potential flow is small.

In the light of the above arguments, we shall linearise the equations of motion (2.20) - (2.22) with respect to departure of velocity from the value just outside the boundary layer. Let us define a new variable, the difference of velocity,

$$u_D = u - U \tag{2.23}$$

where U is the corresponding potential flow velocity, u_D being the difference will be small relative to U.

Substituting (2.23) in (2.20), we get

$$\frac{\partial u_D}{\partial s} + \frac{\partial U}{\partial s} + \frac{\partial v}{\partial n} = 0$$

Neglecting the nonlinear sirst term, we can write

$$\frac{\partial v}{\partial n} = -\frac{\partial U}{\partial s} \tag{2.24}$$

$$v = -\int_0^n \frac{\partial U}{\partial s}\, dn = -nU' \tag{2.25}$$

where prime denotes the differentiation with respect to s.

Equation (2.22) can be written as

$$\frac{\partial}{\partial n}\left(p/\rho + gy\right) = k u^2 \tag{2.26}$$

The equation states that the jump in total pressure, i.e. $p/\rho + gy$ across the boundary layer is of the order and so it can be taken as zero, meaning thereby that the

pressure in the boundary layer is not much different from the pressure in the potential flow as happens in the normal rigid wall boundary layer case. Hence we can write

$$\left[p/\rho + gy\right]_\delta - \left[p/\rho + gy\right]_0 = 0 \qquad (2.27)$$

i.e.

$$\left[p/\rho + gy\right]_{pot.flow} - \frac{p_0}{\rho} - g\zeta = 0 \qquad (2.28)$$

Using Bernoulli's equation for potential flow (double body approximation), we get

$$\frac{p_a}{\rho} + \frac{1}{2}(U_\infty^2 - U^2) - \frac{p_0}{\rho} - g\zeta = 0 \qquad (2.29)$$

The normal stress balance at the free surface gives

$$-p_a + \sigma k = -p_0 + 2\mu\left(\frac{\partial v}{\partial n}\right)_0 \qquad (2.30)$$

Eliminating the pressure between equations (2.29) and (2.30) and using equation (2.20), we get

$$\frac{1}{2}(U_\infty^2 - U^2) - g\zeta + \frac{\sigma k}{\rho} + 2\nu u_0' = 0$$

The last term $2\nu U_0'$ will be of the order $O(\delta^2)$ because of ν and therefore we can replace U_0' by U' or the term can be dropped once and for all. Hence, finally the above equation can be written as

$$\frac{1}{2}(U_\infty^2 - U^2) - g\zeta + \sigma k/\rho + 2\nu U' = 0 \qquad (2.31)$$

Writing $k = \zeta''$ and rearranging, we get

$$\frac{\sigma}{\rho}\zeta'' - g\zeta = -\frac{1}{2}(U_\infty^2 - U^2) - 2\nu U'$$

This equation determines free surface heights independent of the other equation. Thus free surface curvature which occured as one of the variable can now be independently determined. Using U_∞ and r (cylinder-radius) to scale the velocity and distances respectively, we can write

$$\frac{2\zeta''}{W} - \frac{1}{2F^2}\zeta = -\frac{1}{2}(1 - U^2) - \frac{4}{R_e}U' \qquad (2.32)$$

where $F = \dfrac{U_\infty}{\sqrt{g \cdot 2r}}$, $R_e = \dfrac{U_\infty \cdot 2r}{\nu}$, $W = \dfrac{\rho U_\infty^2 \cdot 2r}{\sigma}$

are respectively Froude, Reynolds and Weber numbers. It may be noted here that the curvature of the free surface will dpend upon F, Re and W.

Since the pressure variation in the boundary layer is negligible, the pressure in the boundary layer can be replaced by the pressure in the potential flow. Therefore, with $u=0$, $v=0$ we get from the momentum equation (2.21)

$$U\frac{\partial U}{\partial s} = -\frac{\partial}{\partial s}(p/\rho + gy) \tag{2.33}$$

Substituting equation (2.33) in (2.21), the momentum equation becomes

$$u\frac{\partial u}{\partial s} + v\frac{\partial u}{\partial n} + kuv - U\frac{\partial U}{\partial s} = \nu\frac{\partial^2 u}{\partial n^2} \tag{2.34}$$

Now, introducing the velocity difference variable u_D as defined by equation (2.23) into equation (2.34) and neglecting nonlinear terms in u_D, we get

$$U u_D' + u_D U' + v\frac{\partial u_D}{\partial n} + k u_D v + k U v = \nu\frac{\partial^2 u_D}{\partial n^2} \tag{2.35}$$

The influence of the term $k u_D v$ will be very small compared to the term kUv and therefore the term can be dropped. However, we shall retain the term for the time being. Eliminating v with the help of equation (2.25),

the above equation can be written as

$$\frac{\partial(u_D U)}{\partial s} - nU'\frac{\partial u_D}{\partial n} - ku_D nU' - kU nU' = \nu \frac{\partial^2 u_D}{\partial n^2} \tag{2.36}$$

2.3 Momentum integral equation

Integrating equation (2.36) with respect to n over the boundary layer thickness, we can write

$$\frac{d}{ds}\int_0^\delta U u_D\, dn - U'\int_0^\delta n\frac{\partial u_D}{\partial n}\, dn - kU'\int_0^\delta n u_D\, dn - kUU'.\frac{\delta^2}{2} = \nu\left[\frac{\partial u_D}{\partial n}\right]_0^\delta \tag{2.37}$$

The integral

$$\int_0^\delta n\frac{\partial u_D}{\partial n}\, dn = [n u_D]_0^\delta - \int_0^\delta u_D\, dn = -\int_0^\delta u_D\, dn \quad (\text{as } u_D = 0 \text{ at } n=\delta) \tag{2.38}$$

and let

$$\int_0^\delta n u_D\, dn = D. \tag{2.39}$$

Further, we introduce displacement thickness of boundary layer defined as

$$U\delta_1 = \int_0^\delta (U-u)\,dn \quad = -\int_0^\delta u_D\,dn \tag{2.40}$$

Introducing the expressions (2.38) - (2.40) into equation (2.37), it becomes

$$\frac{d}{ds}(U^2\delta_1) + UU'\delta_1 + kU'D + kUU'\frac{\delta^2}{2} = -\nu\left[\frac{\partial u_D}{\partial n}\right]_0^\delta$$

which simplifies further to give

$$U^2\delta_1' + 3UU'\delta_1 + kU'D + kUU'\frac{\delta^2}{2} = -\nu\left[\frac{\partial u_D}{\partial n}\right]_0^\delta \tag{2.41}$$

Equation (2.41) is the required momentum integral equation with δ_1 defined by (2.40), U, U' and k being known from the potential flow and equation (2.32).

2.4 Velocity profile and evaluation of integrals

Following the standard Kàrmàn-Pohlhausen procedure for boundary layers, we assume the velocity profile for the boundary layer as

$$u_D = U\left[a + b\frac{n}{\delta} + c\frac{n^2}{\delta^2} + d\frac{n^3}{\delta^3}\right] \tag{2.42}$$

At $n = 0$, we get $u_{D_0} = aU$, so the coefficient a is a nondimensional velocity defect in the free surface. The coefficients a , b , c and d can be determined by the boundary conditions which are as follows

(i) $u = U$ i.e. $u_D = 0$ at $n = \delta$ (2.43)

(ii) vorticity = 0 at $n = \delta$ (2.44)

From equation (2.6),

$$\omega = \frac{1}{h_1}\left\{\frac{\partial v}{\partial s} - \frac{\partial}{\partial n}(h_1 u)\right\}$$

In the light of orders of magnitude listed in equation (2.19), we can write, to the first order,

$$\omega = -\frac{\partial u}{\partial n} - ku$$

The condition (2.44) now yields

$$\frac{\partial u}{\partial n} = -kU \qquad \text{at } n = \delta$$

In terms of the difference variable u_D, we can write the above as

$$\frac{\partial u_D}{\partial n} = -kU \tag{2.45}$$

(iii) Tangential stress = 0 at $n = 0$.

From equation (2.8), the shear stress at the free surface is given by

$$\tau_{sno} = \mu \left[\frac{\partial u}{\partial n} - k u \right]_0$$

Therefore the condition gives

$$\frac{\partial u}{\partial n} = k u \qquad \text{at} \quad n = 0$$

In terms of u_D, we obtain

$$\frac{\partial u_D}{\partial n} = k(u_D + U) \tag{2.46}$$

(iv) The assumed velocity profile should be compatible with the linearised momentum equation (2.35) at the free surface.

The condition yields

$$(U u_D' + u_D U')_{n=0} = \nu \left[\frac{\partial^2 u_D}{\partial n^2} \right]_{n=0} \tag{2.47}$$

Thus these four boundary conditions determine the four coefficients a, b, c and d in the velocity profile.

Substituting the velocity profile (2.42) into the conditions (2.43), (2.45) and (2.46), we obtain respectively

$$a + b + c + d = 0 \tag{2.48}$$

$$b + 2c + 3d = -k\delta \tag{2.49}$$

$$b = k\delta(a+1) \tag{2.50}$$

The condition (2.47) in the same way yields

$$c = \frac{\delta^2 U}{2\nu} a' + 2a \frac{\delta^2 U'}{2\nu} \tag{2.51}$$

Let us define the parameters

$$P_1 = \frac{\delta^2 U'}{2\nu} \quad \text{and} \quad P_2 = k\delta \,, \tag{2.52}$$

which appear as nondimensional combinations in the above equations. The quantities P_1 and P_2 will be acting as nondimensional shape factors. Solving the equations (2.48) to (2.50), we obtain

$$b = P_2 (a+1) \tag{2.53}$$

$$c = -(2P_2 + 3)a - P_2 \tag{2.54}$$

$$d = 2a + P_2 a \tag{2.55}$$

Equating the value of c from the expressions (2.51) and (2.54), we obtain

$$P_1 U a' + (2P_1 + 2P_2 + 3) U' a = -P_2 U' \tag{2.56}$$

The integration of differential equation (2.56) which has variable coefficients will give the coefficient a, and then b, c and d will follow from equations (2.53) to (2.55). Substituting the expressions (2.53) to (2.55) into the velocity profile (2.42) we get

$$u_D = U\left[a(1 - 3\eta^2 + 2\eta^3) + P_2 a(\eta - 2\eta^2 + \eta^3) + P_2(\eta - \eta^2)\right] \tag{2.57}$$

where $\eta = \frac{n}{\delta}$

The integrals in the momentum integral equation (2.41) can now be evaluated as follows

$$\int_0^{\delta} u_D \, dn = \delta \int_0^1 u_D \, d\eta$$

Substituting u_D from the equation (2.57) and evaluating the integral, we obtain

$$\int_0^{\delta} u_D \, dn = U\delta . \frac{1}{12} . \left[6a + P_2 a + 2P_2 \right] \qquad (2.58)$$

Substituting equation (2.58) into the equation (2.40), we can write

$$\frac{\delta_1}{\delta} = - \frac{1}{12} \left[6a + P_2 a + 2P_2 \right] \qquad (2.59)$$

Further, proceeding in a similar manner, the evaluation of the integral in the equation (2.39) gives

$$D = \int_0^{\delta} n u_D \, dn = \delta^2 U D_1$$

$$\text{where } D_1 = \left[\frac{3}{20} a + \frac{1}{15} P_2 a + \frac{1}{12} P_2 \right] \qquad (2.60)$$

The r.h.s. of (2.41) can also be evaluated using the boundary conditions (2.45) and (2.46). This gives

$$\left[\frac{\partial u_D}{\partial n} \right]_0^{\delta} = - kU(a+2)$$

The equation (2.41) can now be written as

$$U\delta_1' + 3U'\delta_1 + kU'D_1\delta^2 + kU'\frac{\delta^2}{2} = \nu k(2+a)$$

where D_1 will be given by (2.60).

Introducing nondimensionalisation with U_∞ and ℓ as done earlier and retaining the same symbols for nondimensionalised variables, the above equation becomes

$$U\delta_1' + 3U'\delta_1 + kU'D_1\delta^2 + kU'\frac{\delta^2}{2} = \frac{4k}{Re}\left(1+\tfrac{1}{2}a\right) \quad (2.61)$$

Multiplying with $\delta_1 \frac{Re}{4}$ throughout, we obtain

$$U\delta_1\delta_1'\frac{Re}{4} + 3U'\delta_1^2\frac{Re}{4} + kU'D_1\delta_1\delta^2\frac{Re}{4} + kU'\frac{\delta_1}{2}\delta^2\frac{Re}{4} = k\delta_1\left(1+\tfrac{1}{2}a\right) \quad (2.62)$$

Defining the new variables as

$$Z = \delta_1^2\frac{Re}{4}, \quad Y = k\delta_1, \quad X = \delta_1^2\frac{Re\,U'}{4}, \quad (2.63)$$

which further give

$$Z' = 2\delta_1\delta_1'\frac{Re}{4}, \quad X = ZU', \quad Y = k\sqrt{\frac{4Z}{Re}}$$

The shape factor in terms of nondimensional variables can be written as

$$P_1 = \delta^2 U' \frac{Re}{4} \quad , \quad P_2 = k\delta \tag{2.64}$$

Introducing the definitions (2.63) and (2.64) into (2.62) the momentum integral equation finally can be written as

$$Z' = \frac{1}{U}\left[Y(2+a) - 6X - YP_1(2D_1+1) \right] \tag{2.65}$$

Squaring the equation (2.59) and introducing the definitions (2.63) and (2.64), we obtain

$$X = \frac{P_1}{144}\left[6a + P_2 a + 2P_2 \right]^2 \tag{2.66}$$

Equation (2.66) is a shape factor relationship. The equation (2.56) with nondimensionalised variables can be written as

$$P_1 U a' + (2P_1 + 2P_2 + 3) U' a = -P_2 U' \tag{2.67}$$

Equations (2.64) to (2.66) constitute the equations of the problem along with the expression (2.57) for the velocity profile. As expected, the boundary layer thickness δ appears no more as a separate variable in the equations. It is incorporated in the shape factors only.

3. SOLUTION OF THE EQUATIONS

The system of equations for the problem now comprises of three equations namely (2.65) to (2.67). We first require to integrate equation (2.67) in order to find the coefficient α and substitute into the remaining two equations. The range of integration for the equations is from $-\infty$ to the body. If the range of integration is divided into small steps so that the coefficients of the equation involving the shape factors P_1 & P_2 which are otherwise functions of the independent variable can be treated as constants for the small step of integration, a particular solution of the equation (2.68) can be written as

$$\alpha = K_1$$

where K_1 is a constant for a step of integration but different for different steps. Substituting the above into equation (2.67), we readily obtain

$$\alpha = K_1 = \frac{-P_2}{2P_1+2P_2+3} \qquad (3.1)$$

The general solution of equation (2.67) is expected to be $\alpha = 0$, the reason being that the general solution will correspond to the equation (2.67) with r.h.s. equal to zero, which means $P_2 = 0$ for the complete range of $-\infty$ to the body. This is possible when either k or δ is zero for the complete range. Both the conditions imply that the vorticity boundary layer does not exist. Hence we take the solution (3.1) as the complete solution of (2.67) (A general solution obtained in Appendix B also leads to the same conclusion) .

Substituting (3.1) into (2.66), the shape factor relationship becomes

$$X = \frac{P_1 P_2^2}{144}\left[\frac{3P_2 + 4P_1}{2P_1 + 2P_2 + 3}\right] \qquad (3.2)$$

3.1 Far field solution

For a step by step integration in the range of $-\infty$ to the cylinder for equation (2.61), one has to start computation from a finite distance far away from the cylinder. This will necessitate starting values of the variables which can be obtained from a far field solution. Taking the fact into account that curvature k and the gradient U' are small quantities in the far field, we can neglect the contribution of the terms $kU'D_1\delta^2$ and $kU'\frac{\delta^2}{2}$ relative to the other terms. Further

in the r.h.s., the term $\frac{1}{2}\alpha$, α being the nondimensional velocity difference at the free surface, can be dropped compared to unity. Thus the equation (2.61) in the far field can be approximated as

$$U\delta_1' + 3U'\delta_1 = \frac{4k}{R} \tag{3.3}$$

A general solution will correspond to the equation

$$U\delta_1' + 3U'\delta_1 = 0 \tag{3.4}$$

whose solution obviously can be written as

$$\delta_1 = \frac{c^*}{U^3} \tag{3.5}$$

where c^* is the constant of integration. Since $\delta_1 = 0$ at $x = -\infty$ and $U = U_\infty$ there, so we conclude that $c^* = 0$. Hence $\delta_1 = 0$ is the general solution of the far field equation.

This may further be supported with the observation that equation (3.4) corresponds to $k = 0$ i.e. flat free surface for which the boundary layer phenomenon does not exist. For a particular solution, we first require to

substitute the expressions for U and U' in the equation (3.3). Since the potential flow determination with a free surface is difficult, we use the velocity field of a fully submerged circular cylinder under the well known double body approximation. Further, in the far field, we assume $s \equiv x$, $k = \frac{\partial^2 \zeta}{\partial x^2}$ and the potential velocity components are evaluated at $y = 0$. The equation (3.3) can then be written as

$$\left(1 - \frac{1}{x^2}\right)\delta_1' + \frac{6}{x^3}\delta_1 = \frac{4}{R_e}\zeta'' \qquad (3.6)$$

An asymptotic solution of the equation (3.6) can be written in powers of $1/x$ as follows:

$$\delta_1 = C_0\zeta' + \frac{C_1}{x} + \frac{C_2}{x^2} + \frac{C_3}{x^3} + \cdots \qquad (3.7)$$

Substituting the above in the equation (3.6), we get

$$\left(1 - \frac{1}{x^2}\right)\left[C_0 k - \frac{C_1}{x^2} - \frac{2C_2}{x^3} - \frac{3C_3}{x^4} - \cdots\right]$$

$$+ \frac{6}{x^3}\left[C_0\zeta' + \frac{C_1}{x} + \frac{C_2}{x^2} + \frac{C_3}{x^3} + \cdots\right] = \frac{4k}{R_e}$$

Equating the various powers of $1/x$ on both sides, we get

$$C_0 = \frac{4}{R_e}$$

$$-C_1 - C_0 k = 0$$

$$-2C_2 + 6C_0\zeta' = 0$$

$$-3C_3 + C_1 + 6C_1 = 0$$

$$-4C_4 + 2C_2 + 6C_2 = 0$$

$$- - - - - - - - - - - - - - -$$

$$- - - - - - - - - - - - - - -$$

The solution of above equations gives

$$C_0 = \frac{4}{R_e}, \quad C_1 = -C_0 k, \quad C_2 = 3C_0\zeta',$$

$$C_3 = -\frac{7}{3}C_0 k, \quad C_4 = 6C_0\zeta' \quad \text{and so on.} \tag{3.8}$$

The far field solution can now be written as

$$\delta_1 = \frac{4}{R_e}\left[\zeta' - \frac{k}{x} + \frac{3\zeta'}{x^2} - \frac{7}{3}\frac{k}{x^3} + \frac{6\zeta'}{x^4} - \cdots\right] \tag{3.9}$$

The solution (3.9) gives the value of δ_1 at any point far away from the body which can be made a starting point of the step by step integration procedure.

3.2 Free surface calculation

The slope and curvature of the free surface will be determined by equation (2.32). For the sake of simplification, we shall assume that the influence of Reynolds number and Weber number is small compared to that of Froude number as the first two are large compared to the third. Hence dropping the Reynolds number and Weber number associated terms, the equation (2.32) becomes

$$\zeta = F^2(1 - U^2) \tag{3.10}$$

The above assumption amounts to ignoring the force of surface tension and normal viscous stress on the free surface rise relative to the force of gravity, or in other words the pressure jump across the free surface is taken as zero. This assumption sounds reasonable as a first approximation of the free surface.

For the potential flow velocity field to be used in the equation (3.10), we shall use the velocity components of double body flow, following Patel (1985). Hence, if U_1 and V_1 are the nondimensional velocity components of potential flow past a fully submerged circular cylinder, the equation (3.10) gives

$$\zeta = F^2(1 - U_1^2 - V_1^2) \tag{3.11}$$

at the free surface, where

$$U_1 = 1 - \frac{1}{x^2+y^2} + \frac{2y^2}{(x^2+y^2)^2}$$

$$V_1 = \frac{-2xy}{(x^2+y^2)^2} \tag{3.12}$$

Differentiation of the equation (3.11) with respect to x gives

$$\zeta_x = -F^2(2UU_{1x} + 2VV_{1x}) \tag{3.13}$$

$$\zeta_{xx} = -2F^2(U_1U_{1xx} + U_{1x}^2 + V_1V_{1xx} + V_{1x}^2) \tag{3.14}$$

$$k = \frac{\zeta_{xx}}{(1+\zeta_x^2)^{3/2}} \tag{3.15}$$

where subscript x stands for differentiation.

For the evaluation of the expressions (3.13) and (3.15) for slope and curvature respectively, the velocity components and their derivatives are evaluated at $y=0$ following the usual linearisation of the free surface. The free surface so obtained however does not satisfy any kinematic condition.

3.3 Starting values and computation procedure

We decide a starting point far away from the cylinder and evaluate δ_1 from the far field solution (3.9) with input values of slope and curvature calculated from the expressions (3.13) to (3.15). Thus knowing the value of δ_1, we calculate Z and subsequently X and Y at the starting point using the definition (2.63). The shape factors P_1 and P_2 are related as

$$P_1 = -\frac{P_2^2}{c_s} \quad , \quad c_s = \frac{4}{R_c}\frac{k^2}{|U'|}$$

Elimination of P_1 from the shape factor relation (3.2) leads to a polynomial (8th degree) in P_2 which when solved gives six complex roots and two real roots, one positive and one negative. We select the positive root of P_2 as it leads to a negative value of velocity defect a in equation (3.1) as expected, while the negative root leads

to a positive value of α meaning thereby that the free surface moves faster than the potential flow underneath which is not plausible. Now, knowing P_2, P_1, α we find the value of D_1 from equation (2.60).

The values of $Z, X, Y, P_1, P_2, \alpha$ and D_1 thus calculated serve as starting values for the numerical integration of the momentum integral equation (2.65). Choosing a reasonable step length one calculates Z at the next point. Knowing a fresh value of Z, one can go backward and calculate the corresponding fresh values X, Y, P_1, P_2, α and D_1 using the definitions (2.63), the equation (3.2), (3.1) and (2.60). Thus the boundary layer velocity difference profile can be calculated at each step knowing the values of P_1, P_2 and α from the equation (2.57) and can be converted to boundary layer velocity profile by the simple transformation $u = u_D + U$. Similarly the free surface velocity $u_0 = \alpha U + U$ can also be calculated at each step.

4. RESULTS AND DISCUSSION

4.1 Free surface

The height of the free surface and its slope are computed from equation (3.8) and (3.10) respectively and shown in Figs. 5 and 6. As expected from the double body

approximation, the free surface acquires maximum height at the intersection with the cylinder in accordance with Bernoulli's equation and its slope goes to zero there. The curvature of the free surface is computed from expression (3.12) and used for subsequent calculation. It is positive far away from the body, increases steadily as the computation moves towards the body, attains a maximum, decreases and crosses to the negative side (Table 1) and remains negative for the remaining distance upto the cylinder. This free surface does not satisfy any kinematic condition.

4.2 Boundary layer velocity profile and separation

The velocity difference (u_D) profile computed from equation (2.57) is transformed to boundary layer velocity profile using the transformation (2.23). Fig. 7 shows the profile at different positions ahead of the cylinder for a fixed value of Froude number of 0.5. The computation was started from a point ten radii away from the cylinder with radius 0.05 m (Honji 1976). From the diagram one finds that the velocity profile at 1.21 radius away from the centre of the cylinder has already developed a velocity defect at free surface of about 7% of the corresponding potential flow velocity at this position. The defect in velocity increases as the profile moves closer to the cylinder, being 25% at 1.11 radius, 48% at 1.08 radius and 83% at

1.06 radius. Ultimately the free surface velocity becomes negative somewhere between 1.06 and 1.05 radii away from the cylinder indicating the existence of a free surface separation point (FSSP), the start of back flow and thus the formation of bow vortices. The boundary layer velocity profiles (Fig. 7) show a regular increase in shear resulting finally in separation. However, separation occuring exceedingly close to the cylinder does not agree with the existing experimental observations, Figs.(2 and 3), where it is observed to occur about two radii away from the cylinder. On the other hand, Fig. 8 which gives the variation in the free surface velocity with distance from the cylinder for different Froude numbers, shows that FSSP moves away from the cylinder with increase in Froude number, i.e. the zone of bow vortices increases with increase in Froude number. This fact is in full agreement with the observation of Honji (Fig. 2), Kayo et al. (Fig. 3) and the simple theoretical calculation of Patel (Figs. 2,3). This shows that though the position of FSSP does not agree with the experiments, the results obtained from the proposed model are consistent. It is to be emphasised that the proposed model suceeds as shear flow-model for bow vortices phenomenon and confirms that the bow vortices originate from the action of viscous forces on the curved free surface ahead of the body as pointed out by Patel (1985). The regular increase in shear in the free surface boundary layer (Fig. 7) with decrease in distance from the cylinder supports the calculation of vorticity amplification by Mori (1984) using Lighthill's (1956) drift theory.

One of the reasons for occurrence of FSSP so close to the cylinder may lie in the fact that we have used a non-realistic free surface in the sense that it does not satisfy any kinematic condition and further does not include the effect of surface tension and viscous forces along with gravity. On the other side, the occurrence of FSSP is linked with high curvature and in the present case, high values of curvature occur only exceedingly close to the body. In reality, the free surface ahead of the body will have capillary waves whose amplitude decays to zero due to viscosity. The curvature of the free surface therefore will be high even far ahead due to the undulations of the capillary waves. This is likely to influence the position of free surface separation point. An attempt is made in following sections to find such a free surface in the frame work of wave theory.

4.3 Displacement thickness

Table 1 gives the numerical values of nondimensional displacement thickness δ_1, shape factors P_1 and P_2, velocity defect and curvature, at various positions. It may be observed that displacement thickness increases regularly as the computation progresses towards the cylinder. Velocity defect ultimately becomes more than unity indicating back flow. The starting point of computation was varied from -10 to -15, -20, but there was no significant effect on the position of separation point. In fact the velocity

gradient of potential flow is very low far ahead (e.g. at $x = -10, U = .99$) and that is why shifting the computation point further away from the cylinder does not have a significant effect.

4.4 Role of surface tension

It may be interesting to discuss the role played by surface tension in the generation of bow vortices. The present analysis shows the existence of a shear layer and bow vortices without surface tension being taken into account. Though the results thus obtained do not numerically agree with experimental observations, they show a consistent trend. However, Patel (1985) concludes that surface tension is essential for bow vortices to occur. His calculation which is based upon an approach of selective balance of forces in the normal stress boundary condition results in reasonable values of the position of the separation point; however the momentum equations have not been used by him in arriving at these results. The contradiction in the role played by surface tension invites curiosity. In our opinion, the force of surface tension plays an important role in very low speed cases where the surface contaminants form a stagnant film with surface rigidity that allows a viscous boundary layer to grow underneath, Harper and Dixon (1974), Scot (1982). The position of FSSP is far ahead of the body in these cases and also unpredictable owing to the variation of the surface density of contaminants.

The above phenomenon ceases to play a significant role at moderate speeds. Surface tension being a force normal to the free surface mainly influences its curvature and has little effect on the retardation of the free surface. Even this modification of the free surface shape due to surface tension is small as the shape is predominantly decided by gravity. Therefore, at moderate speeds the influence of surface tension on FSSP, either through modification of free surface curvature or otherwise, is very small. However, this is only a conjecture and must be proved by analysis.

5. ATTEMPTS FOR IMPROVEMENT OF MODEL

5.1 Free surface satisfying kinematic condition

One of the drawbacks in the free surface calculation of the last section is that the free surface does not satisfy any kinematic condition. Patel (1985) has derived the free surface under the same assumptions, i.e. surface tension and viscous force are neglected and potential flow velocity components are taken from double body flow evaluated at the undisturbed level, but additionally, the kinematic condition is satisfied. We calculated the slope and curvature of the free surface from his expressions, equation 25 of Patel (1985) and used them in our calculation of the boundary layer velocity profile. Unfortunately, there was no significant improvement in the results.

5.2 Free surface calculation from wave theory

The free surface ahead of a body, in reality comprises of a gravity wave running upto half the wavelength ahead of the body and joining the capillary waves whose amplitude decays to zero because of viscosity far ahead of the body. Such a wave system will be stationary to an observer moving with the body provided the velocity of the body is more than the minimum velocity of wave generation given by $C_m^2 = 2\sqrt{g\sigma/\rho}$. For an air water interface, this value is .23 m/sec, which corresponds to a Froude number .2322 for the experiments of Kayo, Takekuma, Sharma, Eggers (1982). This is the approximate value beyond which the experiments start giving a definite trend of separation point distance.

An analytic description of such a system is given in Lamb (1932), Art 270 where the wave system is generated by the motion of an integral pressure distribution, Fig. 9.

The expressions for wave elevation are given as follows

$$y = \frac{-2\pi}{(k_2 - k_1)} \frac{P}{\sigma_1 \pi} \sin k_1 x + F(x), \quad x > 0 \tag{5.1}$$

$$y = \frac{-2\pi}{(k_2 - k_1)} \cdot \frac{P}{\sigma_1 \pi} \sin k_2 x + F(x), \quad x < 0 \tag{5.2}$$

where $\sigma_1 = \sigma/\rho$,

$$F(x) = \frac{1}{(k_2-k_1)}\left\{\int_0^\infty \frac{\cos kx}{k+k_1}\,dk - \int_0^\infty \frac{\cos kx}{k+k_2}\,dk\right\} \quad (5.3)$$

Further P defined as

$$P = \int_{-\infty}^{\infty} f(x)\,dx \quad (5.4)$$

is an integral pressure and $f(x)$ is a function, which is zero everywhere except at the origin where it is infinite in the sense that its integral over a narrow band dx is finite and equal to P. The wave numbers k_1, k_2 are given by

$$k_1, k_2 = \frac{U_\infty^2 \pm \sqrt{U_\infty^4 - 4\sigma_1 g}}{2\sigma_1} \quad (5.5)$$

Besides the difficulty to find an appropriate pressure distribution whose streamlines should generate the body, the approach gives a wave system ahead of the body whose amplitude does not decay as there is no dissipation mechanism such as viscosity taken into account.

In order to incorporate viscous effects into the wave system, one requires to find the wave solution for the Navier-Stokes equations, which is difficult. Wu and

Messick (1958) have solved the linearised Oseen's equation and investigated the viscous effect on surface waves generated by steady disturbances in the two dimensional case. Cumberbatch (1965) extended the analysis to the three dimensional case so as to include ship waves. Following the method of Wu and Messick (1958), we shall attempt to find the free surface profile and velocity components for using in our boundary layer calculation in this section.

5.3 Formulation

Consider a uniform stream with velocity U_∞ in the direction of positive x-axis taken on the undisturbed free surface, Fig. 10. Let u and v be the velocity components of a disturbance in the x and y directions respectively. The total velocity vector of the flow can therefore be written as

$$U_\infty + \vec{q} = U+u, v \tag{5.6}$$

$$\operatorname{div} \vec{q} = u_x + v_y = 0, \ |x| < \infty, \ y < 0. \tag{5.7}$$

where the subscripts denote partial derivatives.

For disturbance which is small relative to U_∞ i.e. $|q| << U_\infty$, the linearised Oseen's equation gives

$$U_\infty u_x = -\frac{1}{\rho} p_x + \nu \nabla^2 u \tag{5.8}$$

$$U_\infty v_x = -\frac{1}{\rho} p_y + \nu \nabla^2 v - g \tag{5.9}$$

The kinematic boundary condition on the free surface $y = \zeta(x)$, after usual linearisation may be expressed as

$$U_\infty \zeta_x = v(x,0) \tag{5.10}$$

The normal stress and shear stress boundary conditions duly linearised can be expressed as

$$p(x,0) - 2\mu v(x,0) + \sigma_1 \rho \zeta_{xx} = P(x) \tag{5.11}$$

$$\mu [u_y(x,0) + v_x(x,0)] = Q(x) \tag{5.12}$$

where P denotes the external pressure (or normal stress acting in the y-direction, with the sign reversed), Q is the external shearing stress acting in the x-direction

and μ is the coefficient of viscosity.

The linearised flow $(\vec{q}, p)$ is decomposed into two parts - one irrotational $(\vec{q}_1, p)$ and other solenoidal $(\vec{q}_2, 0)$. Thus we can write

$$\vec{q} = \vec{q}_1 + \vec{q}_2 \quad , \tag{5.13}$$

$$\text{curl } \vec{q}_1 = 0 \quad , \tag{5.14}$$

$$\text{div } \vec{q}_2 = 0 \quad . \tag{5.15}$$

Substituting the equation (5.13) into the equations of motion, (5.8) and (5.9), written in vector form and separating irrotational and solenoidal parts, we obtain

$$U_\infty \frac{\rightarrow}{q_{1x}} = -\nabla (p/\rho + gy) \tag{5.16}$$

$$U_\infty \frac{\rightarrow}{q_{2x}} = \nu \nabla^2 \vec{q}_2 \tag{5.17}$$

Introducing the velocity potential and stream function defined as

$$\vec{q}_1 = \nabla\varphi = (\varphi_x, \varphi_y), \tag{5.18}$$

$$\vec{q}_2 = (\psi_y, -\psi_x), \tag{5.19}$$

where φ satisfies the Laplace equation

$$\varphi_{xx} + \varphi_{yy} = 0, \quad |x| < \infty, \quad y < 0 \tag{5.20}$$

into the equations (5.16) and (5.17) and integrating, we obtain

$$p/\rho = -U\varphi_x - gy, \tag{5.21}$$

$$\psi_{xx} + \psi_{yy} = \frac{U}{\nu}\psi_x \tag{5.22}$$

Introducing the velocity potential and stream function (5.18 - 5.19) into the boundary conditions (5.10) - (5.12) and eliminating $p(x,0)$ from (5.11) using (5.21) at the same time, we finally obtain the boundary conditions

$$U_\infty \zeta_x = \varphi_y - \varphi_x \quad \text{on } y = 0 \tag{5.23}$$

$$U\varphi_x + g\zeta - \sigma_1 \zeta_{xx} - 2\nu(\varphi_{xx} + \psi_{xy}) = -\frac{P(x)}{\rho}, \quad (5.24)$$

$$\nu(2\varphi_{xy} + \psi_{xy} - \psi_{xx}) = \frac{Q(x)}{\rho}, \text{ on } y = 0 . \quad (5.25)$$

The problem is now formulated. We require to solve equations (5.20) and (5.22) subject to the boundary conditions (5.23) - (5.25) for the variables φ, ψ and surface elevation ζ .

5.4 Solution by Fourier transform technique

Defining the Fourier transform pair as

$$\tilde{f}(k) = \int_{-\infty}^{\infty} e^{-ikx} f(x)\, dx \quad (5.26)$$

$$f(x) = \frac{1}{2\pi} \int_{-\infty}^{\infty} e^{ikx} \tilde{f}(k)\, dk \quad (5.27)$$

and introducing the transforms into the equations (5.20) and (5.22), we obtain

$$\tilde{\varphi}_{yy} - k^2 \tilde{\varphi} = 0 \quad (5.28)$$

$$\tilde{\psi}_{yy} - \left(k^2 + \frac{U}{\nu} ik\right) \tilde{\psi} = 0 \qquad (5.29)$$

The solutions for the above equations can be written as

$$\tilde{\varphi} = A(k)\, e^{|k| y}, \qquad (5.30)$$

$$\tilde{\psi} = B(k)\, e^{y\left(k^2 + iUk/\nu\right)^{1/2}} \quad \text{for } y \leq 0 . \qquad (5.31)$$

provided $\left(k^2 + iUk/\nu\right)^{1/2}$ is defined to have its real part positive for k real. The functions $A(k)$ and $B(k)$ can be determined from the transforms of the boundary conditions. Eliminating ζ from the equation (5.24) using the equation (5.23), we get

$$U\varphi_{xx} + (\varphi_y - \varphi_x)\frac{g}{U} - \frac{\sigma}{U}(\varphi_{yxx} - \psi_{xxx}) - 2\nu(\varphi_{xxx} + \psi_{xxy}) = -\frac{P(x)}{\rho} \qquad (5.32)$$

Taking the Fourier transform of the above, it becomes, with some rearrangement

$$\tilde{a}_1 A + \tilde{b}_1 B = \tilde{c}_1 \qquad (5.33)$$

where

$$\tilde{a}_1 = |k|(g+\sigma_1 k^2) - U_\infty^2 k^2 + 2i\nu U_\infty k^3$$

$$\tilde{b}_1 = -ik\left[(g+\sigma k^2) + 2i\nu U_\infty k\left(k^2 + \frac{iUk}{\nu}\right)^{1/2}\right]$$

$$\tilde{c}_1 = -\frac{1}{\rho} \cdot iU_\infty k\tilde{P}$$

(5.34)

Similarly, taking the transform of (5.25), we obtain

$$\tilde{a}_2 A + \tilde{b}_2 B = \tilde{c}_2 \qquad (5.35)$$

where

$$\tilde{a}_2 = 2i|k|$$

$$\tilde{b}_2 = (2k + iU/\nu)$$

$$\tilde{c}_2 = \tilde{Q}/\rho\nu k$$

(5.36)

Solving the above simultaneous equations, we get

$$A = \frac{\tilde{b}_1 \tilde{c}_2 - \tilde{c}_1 \tilde{b}_2}{D_N}$$

$$B = \frac{\tilde{a}_2 \tilde{c}_1 - \tilde{a}_1 \tilde{c}_2}{D_N} \qquad (5.37)$$

where

$$D_N = \tilde{a}_1 \tilde{b}_2 - \tilde{b}_2 \tilde{a}_1$$

The denominator of equations (5.36) and (5.37) can be simplified to give

$$D_N = \frac{i U_\infty |k|}{\nu} \left[(g + \sigma_1 k^2) - |k| (U_\infty - 2i\nu k)^2 - 4k^2 \nu^2 \left(k^2 + \frac{iUk}{\nu}\right)^{1/2} \right] \qquad (5.38)$$

Further, the numerator of equation (5.36) can be expressed as

$$\tilde{b}_1 \tilde{c}_2 - \tilde{c}_1 \tilde{b}_2 = A_1 \tilde{P} + \tilde{A}_2 Q \qquad (5.39)$$

where

$$A_1 = \frac{i U_\infty k}{\rho}\left(2k + \frac{i U_\infty}{\nu}\right)$$

$$A_2 = -\frac{i}{\rho\nu}\left\{(g + \sigma_1 k^2) + 2i U_\infty \nu k\left(k^2 + \frac{i U_\infty k}{\nu}\right)^{1/2}\right\}$$

(5.40)

Similarly the numerator of equation (5.37) can be written as

$$\tilde{a}_2\tilde{c}_1 - \tilde{c}_2\tilde{a}_1 = B_1\tilde{P} + B_2\tilde{Q}$$

where

$$B_1 = 2|k|k\frac{U_\infty}{\rho}$$

$$B_2 = -\frac{1}{\rho\nu k}\left\{|k|(g + \sigma_1 k^2) - U_\infty^2 k^2 + 2i\nu U_\infty k^3\right\}$$

(5.41)

Hence the simplified expressions for the functions A and B can now be written as

$$A = \frac{A_1\tilde{P} + A_2\tilde{Q}}{D_N} \qquad (5.42)$$

$$B = \frac{B_1 \tilde{P} + B_2 Q}{D_N} \tag{5.43}$$

Applying the Fourier transform to equation (5.23), we obtain

$$\tilde{\zeta}(k) = \frac{|k| A - ikB}{ikU_\infty} \tag{5.44}$$

The integral representation of $\zeta(x)$ can be obtained by taking the inverse transform of the equation (5.44). This then gives

$$\zeta(x) = \frac{1}{2\pi}\int_{-\infty}^{\infty} e^{ikx} \frac{(|k|A_1 - ik_1 B_1)\tilde{P}_1 + (|k|B_1 - ikB_2)\tilde{Q}}{ikU_\infty D_N} \tag{5.45}$$

Let us define

$$\zeta(x) = H_p(x) \text{ for } P(x) = \tfrac{1}{2}\rho U_\infty^2 G(x),\ Q(x) = 0$$

$$\zeta(x) = H_Q(x) \text{ for } P(x) = 0,\ Q(x) = \tfrac{1}{2}\rho U_\infty^2 G(x) \tag{5.46}$$

where $G(x)$ is a Dirac delta function, i.e. $G(x)=0$ for all x except $x = 0$ where $G(x) = 1$. Thus H_P and H_Q are surface displacements corresponding to the concentrated normal stress and the concentrated shearing stress at the origin respectively. The surface elevation for a distributed pressure and shear stress can now be written by using linear superposition as

$$\zeta(x) = \frac{1}{\rho U_\infty^2}\int_{-\infty}^{\infty}\left\{H_P(x-\xi)\,P(\xi) + H_Q(x-\xi)\,Q(\xi)\right\}d\xi \tag{5.47}$$

For the present problem, we shall take $Q(x) = 0$. Consequently, the surface elevation for a concentrated or distributed normal stress, i.e. expression (5.45), on substitution of A_1 and B_1 from (5.40) and (5.41) respectively and after due simplification yields

$$\zeta(x) = -\frac{1}{2\pi\rho}\int_{-\infty}^{\infty}\frac{e^{ikx}\cdot\tilde{P}(k)}{D_2}\,dk$$

where

$$D_2 = \left[(g+\sigma_1 k^2) - |k|\left\{U_\infty - 2i\nu k\right\}^2 - 4k^2\nu^2\left(k^2 + \frac{iU_\infty}{\nu}k\right)^{1/2}\right] \tag{5.48}$$

Similarly, the solution for φ and ψ can be written from the inverse transforms of equations (5.30) and (5.31), i.e.

$$\varphi(x) = \frac{1}{2\pi}\frac{\nu}{\rho}\int_{-\infty}^{\infty} \frac{\frac{k}{|k|}\, e^{ikx}\,(2k + i\frac{U_\infty}{\nu})\, e^{|k|y}\,\tilde{P}(k)\,dk}{D_2} \tag{5.49}$$

$$\psi(x) = -\frac{2i}{\pi}\frac{\nu}{\rho}\int_{-\infty}^{\infty} \frac{k\, e^{ikx}\, e^{y(k^2 + iU_\infty k/\nu)^{1/2}}\,\tilde{P}(k)\,dk}{D_2} \tag{5.50}$$

The velocity components $U+u, v$ can now be calculated. Since it would be sufficient to get their value at $y = 0$, the equation (5.10) gives

$$v = U_\infty \zeta_x \tag{5.51}$$

which can be calculated knowing ζ_x from (5.48). For the horizontal component, if we ignore the contribution of viscosity, i.e. $\vec{q}_2$, we can write

$$U + u = U + \varphi_x \tag{5.52}$$

where φ_x can be found from equation (5.49).

5.5 Solution for concentrated normal stress

For this case, we require to set $\tilde{P}(k) = \frac{1}{2}\rho U_\infty^2$ (cf. 5.46). Hence, doing so and introducing the following nondimensional quantities,

$$x' = x k_m \quad , \quad k' = k/k_m \, ,$$

$$U_o = \frac{U_\infty}{c_m} \quad , \quad \alpha = \frac{\nu k_m}{U_\infty} \tag{5.53}$$

where c_m and k_m are respectively the minimum phase velocity and the corresponding wave number of waves in a nonviscous medium defined as

$$c_m = (4g\sigma_1)^{1/4} \, , \quad k_m = \left(\frac{g}{\sigma_1}\right)^{1/2}$$

the expression (5.48) gives

$$H_p(x) = -\frac{U_o^2}{\pi} Re \int_0^\infty \frac{e^{ikx'}}{f(k; U_o; \alpha)} \, dk \tag{5.54}$$

where the prime of k has been dropped and

$$f(k;U_0;\alpha) = (k^2+1) - 2U_0 k(1-2i\alpha k)^2 - 8U_0^2\alpha k^2\{\alpha k(\alpha k+i)\}^{1/2} \tag{5.55}$$

The quantity α can be regarded as inverse Reynolds number and is a measure of the relative importance of viscous and inertia effects.

For the case when viscosity is neglected, i.e.

$$f(k;U_0,0) = k^2 - 2U_0^2 k + 1 = 0 \tag{5.56}$$

If k_1 , k_2 are the roots of the above quadratic, we can write

$$k_1 = U_0^2 - (U_0^4-1)^{1/2}, \quad k_2 = U_0^2 + (U_0^4-1)^{1/2} \tag{5.57}$$

Obviously

$$k_2 = \frac{1}{k_1}$$

The function $f(k;U_0;\alpha)$ has two simple zeros on the positive real k-axis at k_1 and k_2 for $U_0 > 1$

or a double zero at $k = 1$ for $U_0 = 1$, or two complex conjugate zeros for $U_0 > 1$. The problem is indeterminate for $\alpha = 0$, but fully determinate otherwise.

5.6 Evaluation of integrals for small α or large Reynolds numbers

Viscous effects can be incorporated by following an approximate procedure of expanding the zeros of in terms of α, about their nonviscous locations, $f(k; U_0; \alpha)$. i.e. writing

$$k_1(U_0, \alpha) = k_{10} + a_1\alpha + b_1\alpha^{3/2} + c_1\alpha^2 + \cdots$$

$$k_2(U_0, \alpha) = k_{20} + a_2\alpha + b_2\alpha^{3/2} + c_2\alpha^2 + \cdots$$

(5.58)

Substituting in the equation $f(k; U_0; \alpha) = 0$ and equating the coefficients of the various powers of α, we can write the values of the coefficients as

$$a_1 = \frac{4i U_0^2 k_{10}^2}{(U_0^4 - 1)^{1/2}}, \qquad a_2 = \frac{4i U_0^2 k_{20}^2}{(U_0^4 - 1)^{1/2}}$$

$$b_1 = \frac{e^{-i\pi/4} \cdot 4U_0^2 k_1^{5/2}}{(U_0^4-1)^{1/2}}, \quad b_2 = \frac{e^{i\pi/4} \cdot 4U_0^2 k_2^{5/2}}{(U_0^4-1)^{1/2}}$$

(5.59)

We shall restrict ourselves to the case $U_0 > 1$ i.e. $U > c_m$ and α small. For such a case, k_1 will lie in the first quadrant and k_2 in the fourth quadrant. The integrals can now be calculated by the residue theorem. For $x' > 0$, we construct a closed contour Γ consisting of the original path along the real k-axis from $k = 0$ to $k = R_1$, a circular arc of large radius $|k| = R_1$ in the first quadrant and the return along the imaginary axis from $k = iR_1$ back to the origin. Then Γ encloses one simple pole $k = k_1$ given by the equation (5.58) for $0 < \alpha < 1$. By letting $R_1 \to \infty$, the contribution along the circular arc vanishes, and the theorem of residues yields, for $x' > 0$

$$H_p(x) = -\frac{U_0^2}{\pi} \mathrm{Re}\left[2\pi i \, \mathrm{Res.}(k_1)\right] + L(x)$$

$$L(x) = -\frac{U_0^2}{\pi} \mathrm{Re} \int_0^{i\infty} \frac{e^{ikx'}}{f(k, U_0, \alpha)} \, dk$$

(5.60)

$$\text{Residue at } k_1 = \frac{e^{ik_1 x'}}{\left(\frac{df}{dk}\right)_{k=k_1}}$$

Differentiation of the equation (5.55) yields

$$\frac{df}{dk} = 2k - 2U_0^2 + O(\alpha)$$

which on substituting k_1 from its expression (5.58) and neglecting the terms of $O(\alpha)$ and above, becomes

$$-2(U_0^4 - 1)^{1/2}$$

Substituting k_1 from (5.58) in the exponent term $\exp[ik_1 x']$, we get

$$\exp[ik_1 x'] = \exp[i(k_{10} + a_1\alpha + b_1\alpha^{3/2} + \cdots)]$$

Substituting the expressions for a_1 and b_1 and retaining terms upto the order $O(\alpha)$, we get

$$\exp[ik_1x'] = \exp\left[i\left(k_{1_0} + \frac{4iU_0^2 k_{1_0}^2 \alpha}{(U_0^4 - 1)^{1/2}}\right)x'\right]$$

which can further be written as

$$= \exp\left[\frac{-4U_0^2 k_{1_0}^2 \alpha x'}{(U_0^4 - 1)^{1/2}}\right] \cdot (\cos k_{1_0}x' + i \sin k_{1_0}x')$$

For the evaluation of the integral $L(x)$, we may put $\alpha = 0$ in the denominator of the integrand as a first approximation. The expression then becomes

$$L(x) = -\frac{U_0^2}{\pi} Rl \int_0^{i\infty} \frac{e^{ikx'}}{(k-k_{1_0})(k-k_{2_0})} dk$$

Making the substitution

$$k = iw$$

$$dk = i\,dw$$

we get

$$L(x) = \frac{U_0^2}{\pi} Rl \int_0^{\infty} \frac{i\,e^{-wx'}}{(w+ik_{1_0})(w+ik_{2_0})} dw$$

Resolving the integrand into partial fractions, we can write

$$L(x') = \frac{U_0^2}{\pi} Rl \cdot \frac{1}{(k_{20} - k_{10})} \int_0^\infty \left\{ \frac{e^{-x'\omega}}{\omega + ik_{10}} - \frac{e^{-x'\omega}}{\omega + ik_{20}} \right\} d\omega$$

Substituting $x'(\omega + ik_{10}) = t$ in the first integral, we get

$$\int_0^\infty \frac{e^{-x'\omega}}{\omega + ik_{10}} d\omega = e^{ik_{10}x} \int_{ik_{10}x}^\infty \frac{e^{-t}}{t} dt = e^{ik_{10}x} \, ei(ik_{10}x)$$

where $ei(z) = \int_z^\infty \frac{e^{-t}}{t} dt$ is a standard integral.

Similarly

$$\int_0^\infty \frac{e^{-x'\omega}}{\omega + ik_{20}} d\omega = e^{ik_{20}x} \cdot ei(ik_{20}x)$$

Hence, we can finally write

$$L(x') = \frac{U_0^2}{\pi} \frac{1}{k_{20} - k_{10}} Rl \left[e^{ik_{10}x'} ei(ik_{10}x') - e^{ik_{20}x'} ei(ik_{20}x') \right] \quad (5.61)$$

The free surface elevation for a point pressure can now be written as

$$H_p(x') = \frac{-U_0^2}{(U_0^4-1)^{1/2}} \exp\left\{\frac{-4U_0^2 k_{10}^2 \alpha}{(U_0^4-1)^{1/2}} x'\right\} \sin k_{10} x' + L(x') \tag{5.62}$$

where $L(x')$ is given by equation (5.61).

For the case of $x' < 0$, i.e. ahead of the pressure point, we can evaluate the integral (5.54) in exactly the same way except that now the closed contour Γ will be the boundary of the fourth quadrant of the k-plane with the branch cut on the imaginary axis lying just outside Γ. For $0 < \alpha < \frac{1}{4}$, Γ shall enclose now only a simple pole at $k = k_2$ given by equation (5.58).

Hence, by the residue theorem, we can write for $x < 0$.

$$H_p(x') = \frac{-U_0^2}{\pi} \mathrm{Re}\left[\left\{2\pi i \cdot \frac{e^{ik_{20}x'}}{\left(\frac{df}{dk}\right)_{k=k_2}}\right\} + \int_0^{-i\infty} \frac{e^{ikx'}}{f(k; U_0, 0)}\, dk\right]$$

Carrying out the process for evaluation and simplification as earlier, we finally obtain

$$H_p(x') = \frac{-U_0^2}{(U_0^4-1)^{1/2}} \exp\left[\frac{4\alpha U_0^2 k_{20}^2 x'}{(U_0^4-1)^{1/2}}\right] \sin k_{20} x' + L(|x'|) \tag{5.63}$$

where $L(|x'|)$ represents the same function $L(x')$ of equation (5.61) with x' replaced by $|x'|$.

For the calculation of velocity potential φ we proceed as follows. Introducing the nondimensional variables as defined in equation (5.53) into the equation (5.49) and setting $\tilde{p}(k) = \frac{1}{2}\rho U_\infty^2$ we get the nondimensional φ as

$$\varphi = \frac{\alpha U_0^2}{\pi} Rl \int_0^\infty \frac{e^{ikx'} \cdot e^{k y} \left(2k + \frac{i}{\alpha}\right) dk}{f(k; U_0; \alpha)} \tag{5.64}$$

For the case of $x' < 0$, using the same procedure of contour integration as followed for the surface elevation $\zeta(x)$, we obtain

$$\varphi(x') = \frac{U_0^2}{\pi} Rl \left[2\pi i \frac{e^{ik_2 x'} \cdot i e^{k_2 y}}{2(U_0^4 - 1)^{1/2}} \right] + \frac{U_0^2}{\pi} Rl \int_0^{-i\infty} \frac{i e^{ikx'} \cdot e^{ky}}{f(k, U_0, 0)} dk \tag{5.65}$$

where $\alpha = 0$ has been substituted in the denominator of the integrand.

Substituting $y = 0$ to evaluate φ on the linearised free surface and following the procedure for the evaluation of $L(x)$, the expression can be finally written as

$$\varphi(x) = \frac{-U_0^2}{(U_0^4-1)^{1/2}} \exp\left\{\frac{4\alpha U_0^2 k_{20}^2 x'}{(U_0^4-1)^{1/2}}\right\} \cos k_{20} x' + L_1(|x'|) \tag{5.66}$$

$$L_1(x') = \frac{U_0^2}{\pi} \mathrm{Rl}.\frac{i}{k_{20}-k_{10}} \left\{ e^{ik_{10}x} ei(ik_{10}x) - e^{ik_{20}x} ei(ik_{20}x) \right\} \tag{5.67}$$

where x' is to be changed to $|x'|$ when substituted.

We shall now simplify the expression for $L(x)$ so as to separate its real and imaginary parts. From the equation (5.61), we have

$$L(x) = \frac{U_0^2}{\pi(k_{20}-k_{10})} \mathrm{Rl}\left[e^{ik_{10}x} ei(ik_{10}x) - e^{ik_{20}x} ei(ik_{20}x) \right] \tag{5.68}$$

where $$ei(z) = \int_z^\infty \frac{-t}{t} dt$$

So $$ei(ik_{10}x) = \int_{ik_{10}}^\infty \frac{-t}{t} dt ,$$

Substituting $t = iu$, so that $dt = i\,du$ we obtain

$$ei(ik_{10}x) = \int_{k_{10}x}^\infty \frac{\cos u}{u} du - i\int_{k_{10}x}^\infty \frac{\sin u}{u} du$$

which can be written as

$$ei(ik_{10}x) = -C_i(k_{10}x) - i\left\{\frac{\pi}{2} - S_i(k_{10}x)\right\}$$

where the functions and are standard integrals defined as

$$C_i(x) = \int_x^\infty \frac{\cos t}{t}\,dt \;,\quad S_i(x) = \int_0^x \frac{\sin t}{t}\,dt$$

The functions C_i and S_i are tabulated function (Abramowitz and Stegun,).

Similarly, we can write

$$ei(ik_{20}x') = -C_i(k_{20}x) - i\left\{\frac{\pi}{2} - S_i(k_{20}x)\right\}$$

Substituting the above back into equation (5.68) and simplifying, we finally obtain

$$L(x) = \frac{U_0^2}{2\pi(U_0^4-1)^{1/2}}\left[D(k_{10}x') - D(k_{20}x')\right]$$

where

$$D(k_{j_0}x') = -\cos(k_{j_0}x')\,C_i(k_{j_0}x') + \sin k_{j_0}x'\left\{\frac{\pi}{2} - S_i(k_{j_0}x')\right\}_{j=1,2} \qquad (5.69)$$

Further, the expression (5.62) for the elevation can be written as

$$\zeta(x') = -A_0 \exp\{B_0 x'\}\sin k_{2_0}x' + \frac{A_0}{2\pi}\left[D(k_{1_0}x) - D(k_{2_0}x)\right] \qquad (5.70)$$

where $A_0 = \dfrac{U_0^2}{(U_0^4-1)^{1/2}}$, $B_0 = 4\alpha A_0 k_{2_0}^2$

D is defined by equation (5.69), and $\zeta(x)$ is used in place $H_p(x)$.

The appearance of α in B_0 characterises viscous damping of amplitude. For the calculation of the derivative ζ_x we require to differentiate the above expression with respect to x . The differentiation of the free wave part is straight forward. For the differentiation of the special functions C_i and S_i in the local wave part we proceed as follows

$$C_i(k_{j_0}x) = -\int_{k_{j_0}x}^{\infty}\frac{\cos u}{u}\,du = -\left[F(\infty) - F(k_{j_0}x)\right]$$

where $F(u) = \int \frac{\cos u}{u}\, du$, $\frac{dF}{du} = \frac{\cos u}{u}$

$$\frac{d}{dx}\left[C_i(k_{j_0}x)\right] = \frac{\cos k_{j_0}x}{x} = f_1 \text{ say} \tag{5.71}$$

$$\frac{d^2}{dx^2}\left[C_i(k_{j_0}x)\right] = -k_{j_0}\frac{\sin k_{j_0}}{x} - \frac{\cos k_{j_0}x}{x^2} \tag{5.72}$$

$$= f_3 \text{ say} \quad , \qquad j = 1,2$$

Further

$$\frac{\pi}{2} - S_i(k_{j_0}x) = \int_{k_{j_0}x'}^{\infty} \frac{\sin u}{u}\, du$$

In the same way

$$\frac{d}{dx}\left[\frac{\pi}{2} - S_i(k_{j_0}x)\right] = -\frac{\sin k_{j_0}x}{x} = f_2 \text{ say} \tag{5.73}$$

$$\frac{d^2}{dx^2}\left[\frac{\pi}{2} - S_i(k_{j_0}x)\right] = -\frac{k_{j_0}\cos k_{j_0}x}{x} + \frac{\sin k_{j_0}x}{x^2} \tag{5.74}$$

$$= f_4 \text{ say}$$

Now we can write the expressions for derivatives as follows

$$\zeta_x(x') = -k_{10}A_0 \exp\{B_0 x'\}\cos k_{20}x' + L_2(|x'|) \tag{5.75}$$

where

$$L_2(x) = \frac{A_0}{2\pi}\Big[F_2(k_{1_0}x) - F_2(k_{2_0}x)$$

$$F_2(k_{j_0}x) = k_{j_0} \sin k_{j_0}x \; C_i(k_{j_0}x) - \cos(k_{j_0}x).f_1$$
$$+ k_{j_0}\cos(k_{j_0}x)\left\{\frac{\pi}{2} - S_i(k_{j_0}x)\right\}$$
$$+ \sin(k_{j_0}x).f_2 \qquad , j=1,2$$

$$\zeta_{xx} = k_{2_0}^2 A_0 \exp\{B_0 x'\} \sin k_{2_0}x' + L_3(|x'|) \qquad (5.76)$$

where

$$L_3(x) = \frac{A_0}{2\pi}\Big[G_3(k_{1_0}x) - G_3(k_{2_0}x)$$

$$G_3(k_{j_0}x) = k_{j_0}^2 \cos k_{j_0}x \; C_i(k_{j_0}x) + 2k_{j_0} \sin(k_{j_0}x).f_1$$
$$- k_{j_0}^2 \sin k_{j_0}x \left\{\frac{\pi}{2} - S_i(k_{j_0}x\right\}$$
$$+ 2k_{j_0}\cos k_{j_0}x \cdot f_2 + \sin k_{j_0}x \cdot f_4 ,$$
$$j = 1, 2$$

where f_1 . f_2 . f_3 and f_4 are given by the expressions (5.71) to (5.74).

Similarly, we can write from the equations (5.66) and (5.67)

$$\varphi = -A_0 \exp\{B_0 x'\} \cos k_{20} x + L_1(|x'|)$$

where

$$L_1(x) = -\frac{A_0}{2\pi}\left[H_1(k_{10}x) - H_1(k_{20}x)\right]$$

$$H_1(k_{j0}x) = \sin k_{j0}x\, C_i(k_{j0}x) + \cos k_{j0}x\left\{\frac{\pi}{2} - S_i(k_{j0}x)\right\}$$
$$j = 1, 2$$

(5.77)

$$\varphi_x = A_0 k_{20} \sin k_{20} x' \exp\{B_0 x'\} + L_4(|x'|)$$

where

$$L_4(x) = -\frac{A_0}{2\pi}\left[H_2(k_{10}x) - H_2(k_{20}x)\right]$$

$$H_2(k_{j0}x) = k_{j0}\cos k_{j0}x\, C_i(k_{j0}x) - k_{j0}\sin k_{j0}x\left\{\frac{\pi}{2} - S_i(k_{j0}x) + \sin k_{j0}x \cdot f_1 + \cos k_{j0}x \cdot f_2\right\}, \quad j = 1, 2$$

(5.78)

Thus, knowing the derivatives, we can write the nondimensional curvature as

$$k = \frac{\zeta_{xx}}{(1+\zeta_x^2)^{3/2}}$$

and the nondimensional velocity components as

$$U_0 + u, \; v = U_0 + \varphi_x, \; U_0 \zeta_x$$

where the nondimensionalisation refers to the definitions in equation (5.63).

5.7 Observations in computation

The computation of the free surface elevation and the other quantities showed that

(i) The free wave part is oscillatory and waves are steep, as expected in the point pressure case.

(ii) The local wave part is also oscillatory, instead of being monotonic decreasing, as normally expected.

(iii) The viscous decay factor reduces the amplitude of the free wave part as the distance from the body increases.

(iv) The velocity is oscillatory and there is no regular decrease in velocity as the body is approached like in the double body approximation.

On re-examining the analysis for the local wave part, it turned out that the integral $L(x)$ is actually non-oscillatory but was approximated as the product of two oscillatory functions resulting in an oscillatory nature of the local wave part. The steepness of waves is obviously due to the fact that the pressure is concentrated at a point. In the following section, we shall calculate the free surface for a distributed pressure and also calculate the local wave integral by a different method.

The local wave integral $L(\alpha)$ after the transformation to a real variable becomes (cf. equation 5.61)

$$L(x) = \frac{U_0^2}{\pi} Rl\, i \int_0^\infty \frac{e^{-\omega x}}{(\omega + ik_{10})(\omega + ik_{20})} d\omega$$

Multiplying the numerator and denominator of the integrand with $(\omega - ik_{10})(\omega - ik_{20})$, the integral becomes

$$L(x) = \frac{U_0^2}{\pi} Rl\, i \int_0^\infty \frac{e^{-\omega x}(\omega - ik_{10})(\omega - ik_{20})}{(\omega^2 + k_{10}^2)(\omega^2 + k_{20}^2)} d\omega$$

Simplifying the above and taking real part, we obtain

$$L(x) = \frac{A_0}{2\pi} \int_0^\infty \left[\frac{e^{-\omega x}}{\omega^2 + k_{10}^2} - \frac{e^{-\omega x}}{\omega^2 + k_{20}^2} \right] d\omega \qquad (5.79)$$

The integrals in the above can be evaluated by quadrature directly avoiding the undue oscillations in the local wave part.

5.8 Solution for distributed normal stress - flat ship approximation

With the modified form of $L(x)$ as in equation (5.79) we can now write the solution for a concentrated pressure as follows,

$$H_p(x') = A_0 e^{B_0 x} \sin k_{20} x' + \frac{A_0}{2\pi} \left[S(k_{10}, |x'|) - S(k_{20}, |x'|) \right]$$

where

$$S(k_{j0}, |x'|) = \int_0^\infty \frac{e^{-\omega |x'|}}{\omega^2 + k_{j0}^2} d\omega \qquad (5.80)$$

For a distributed pressure, according to equation (5.47), the solution for surface elevation can be written as

$$\zeta(x) = \frac{1}{\frac{1}{2}\rho U_\infty^2}\left[A_0 \int_{-r}^{r} e^{B_0(x-\xi)} \sin\{k_{20}(x-\xi)\}\, P(\xi)\, d\xi \right.$$

$$\left. + \frac{A_0}{2\pi}\int_{-r}^{r}\left\{S\{k_{10},(x-\xi)\} - S\{k_{20},(x-\xi)\}\right\}P(\xi)\, d\xi\right]$$

(5.81)

where $P(\xi)$ is the known pressure distribution function. Since it is extremely difficult to find $P(\xi)$ such that the streamlines will generate contour of the body, we shall resort here to the flat ship approximation. According to the flat ship approximation, for a circular cylinder, Fig. 10:

$$P(\xi) = \frac{\rho g \sqrt{r^2 - \xi^2}}{2r}$$

In terms of the nondimensional variables, the above expression can be written as

$$P(\xi) = \frac{\rho g \sqrt{r_1^2 - \xi^2}}{2r_1} \qquad (5.82)$$

where $r_1 = r k_m$

The circular variation of the above expression can be approximated by a sinusoidal function which will be easier for integration. Hence we can write

$$P(\xi) = \frac{\rho g}{2} \cos b_3 \xi \qquad (5.83)$$

where $$b_3 = \frac{\bar{\lambda}}{2\pi k_m}$$

is the pressure intensity or pressure per unit length.

Let FW and LW denote the free wave and the local wave parts of the expression (5.81) for $\zeta(x)$. Substituting the equation (5.83) in the free wave part of the equation (5.81), we obtain

$$FW = \frac{g}{U_\infty^2} \frac{A_0}{k_m} e^{B_0 x} \int_{-\pi_1}^{\pi_1} e^{-B_0|\xi|} \{\sin k_{20} x \cos k_{20} \xi - \cos k_{20} x \sin k_{20} \xi\} \cos b_3 \xi \, d\xi \qquad (5.84)$$

The variation in $e^{-B_0|\xi|}$ in the range of integration will be small because B_0 is small due to the factor α in it. As a first approximation of the integral, we can take the value of $e^{-B_0|\xi|}$ at $\xi = 0$ to represent the complete range of integration. This leads to the simplified expression

$$FW = \frac{g}{U_\infty^2}\frac{A_0}{k_m} e^{B_0 x'} \int_{-x_1}^{x_1} \sin k_{20} x' \cos k_{20}\xi \cos b_3 \xi \, d\xi \qquad (5.85)$$

The second integral in equation (5.84) will yield zero because of antisymmetry. The expression (5.84) after several algebraic steps finally gives

$$FW = \frac{F^2 \cdot 2\pi A_0}{\pi^2 - 4x_1^2 k_{20}^2} e^{B_0 x} \sin k_{20} x \cos k_{20} x_1 \qquad (5.86)$$

where F is the Froude number defined in equation (2.32).

The local wave part of equation (5.81), for $x < 0$, after substitution of equation (5.83) and simplification gives

$$LW = \frac{g}{U_\infty^2}\frac{A_0}{2\pi k_m} \int_0^\infty \int_{-x_1}^{x_1} e^{\omega(x-\xi)} \left[\frac{1}{\omega^2 + k_{10}^2} - \frac{1}{\omega^2 + k_{20}^2}\right] \cos b_3 \xi \, d\xi \, d\omega \qquad (5.87)$$

This integral can be calculated by quadrature. Thus knowing FW and LW, we can now calculate the surface elevation as

$$\zeta(x) = FW + LW$$

For the derivatives ζ_x and ζ_{xx}, the FW part can be differentiated directly to obtain

$$\frac{d}{dx}(FW) = \frac{F^2 \cdot 2\pi A_0}{\pi^2 - 4r_1^2 k_{20}^2} e^{B_0 x} k_{20} \cos k_{20} x + O(\alpha) \tag{5.88}$$

$$\frac{d^2}{dx^2}(FW) = \frac{F^2 \cdot 2\pi A_0}{\pi^2 - 4r_1^2 k_{20}^2} e^{B_0 x} (-k_{20}^2) \sin k_{20} x + O(\alpha) \tag{5.89}$$

The differentiation of the LW part can be obtained numerically.

For the calculation of φ for distributed pressure, the FW part of expression (5.77) yields

$$\varphi = \frac{-g}{U_\infty^2} \frac{A_0}{k_m - r_1} \int_{-r_1}^{r_1} e^{B_0(x-\xi)} \cos k_2(x-\xi) \cos b_3 \xi \, d\xi \tag{5.90}$$

which, following the identical simplification steps as for $\zeta(x)$, reduces to

$$\varphi = -\frac{F^2 A_0 \cdot 2\pi}{(\pi^2 - 4r_1^2 k_{20}^2)} e^{B_0 x} \cos k_2 x \tag{5.91}$$

The differentiation of the above gives

$$\phi_x = \frac{F^2 A_0 . 2\pi}{(\pi^2 - 4\alpha_1^2 k_{20}^2)} \cdot e^{b_0 x} k_{20} \sin k_{20} x \qquad (5.92)$$

The contribution of the local wave part has to be accordingly computed and added with the above.

5.9 Computations for distributed pressure and discussion

A computation of the free surface profile and other quantities was made. As there was very limited time in hand, the computation of the surface elevation, slope and curvature, and the velocity components was carried out only with the free wave part. The local wave part was not considered with the idea that its contribution far away from the body is anyway small. It was observed that,

(i) The waves are now less steep, with their amplitude decaying because of the viscous decay factor.

(ii) The velocity is oscillatory as is clear from its expressions and there is no velocity gradient like that in double body flow.

(iii) The free surface velocity defect in the free surface shear layer oscillates between very narrow range. The reason for this is certainly the absence of the velocity gradient.

In fact, the present attempt of calculating free surface incorporating the effect of surface tension and viscosity assumes a basic flow as a uniform stream, with a small disturbance because of the presence of the body. The velocity gradient (cf. double body flow) disappears in this approach because of linearisation with respect to disturbance. The velocity is oscillating only about the free stream velocity. Therefore the phenomenon of free surface shear layer for which a velocity gradient is essential is very weak in this case. What is required is to calculate the free surface with capillary waves of decaying amplitude due to viscosity along with the basic flow which is not constant but has a gradient such that the velocity is zero at the body.

Taking the basic flow U not constant but as a function of x, we made an attempt to break up the flow into potential and solenoidal parts as done by Wu and Messick (1958). But this was not found possible (Appendix A).

6. CONCLUDING REMARKS

The problem of free surface flow past a semi-submerged horizontal cylinder is considered. A shear flow model is presented to explain the bow vortices observed by various authors. The vorticity generated by viscous forces acting on the free surface is assumed to be concentrated in a thin

layer at the free surface adjoining the potential flow. The equations of the free surface boundary layer are solved under the assumption that the velocity defect in the free surface is small compared to the corresponding velocity in the potential flow. Free surface velocity and boundary layer profile is computed for a free surface obtained from double body flow.

The computation of boundary layer profile at various positions shows that there is a regular increase in shear in the profiles as the flow approaches the body.

The computed free surface velocity decreases faster than the corresponding potential flow velocity and becomes negative ahead of the body, resulting in back flow characterising bow vortices. The phenomenon occurs at exceedingly close distances from the body which is against the experimental observation. However, the model establishes that the free surface shear layer is the origin of the bow vortices. It is further observed that the free surface boundary layer profiles Fig. 7, have a point of inflexion and become flatter and flatter around this point as the flow approaches the body. It is well known by Rayleigh's theorem in hydrodynamic stability that the velocity profiles with points of inflexion are unstable. It may be apprehended that the bow vortices phenomenon might start much earlier because of the instability of boundary layer profiles than because of free

surface velocity becoming negative which occurs very close to the body. It may therefore be worth making a stability analysis of the boundary layer flow instead of being limited to the calculation of free surface velocity.

A second possibility of improvement of the model may be sought in the use of a more realistic characterisation of the free surface incorporating surface tension and viscous effects. In this regard, the free surface and the potential flow velocities were calculated by the method of Wu and Messick (1958) which incorporates surface tension and viscous decay. It was expected that the high curvature in capillary waves will improve the separation criterion, but the attempt was not successful because of the fact that the waves were taken as a disturbance on a uniform stream which obscured the presence of the velocity gradient in the basic flow responsible for the growth of the free surface shear layer. It was not possible to use the technique of Wu and Messick (1958) for the basic flow which is not constant but has a gradient.

A third possibility of improving upon the model may be found in doing away with the assumption of small free surface velocity defect compared to potential flow velocity. This will increase the nonlinearity in the equations and require the introduction of momentum thickness into them. The attempt is in progress.

It is concluded that the free surface shear layer phenomena explain the existence of bow vortices in two dimensions and deserves further investigation to explain the vortices ahead of ship models.

APPENDIX A

Let the velocity vector be

$$U + \vec{q} = U + u, v \qquad (1)$$

where U is not constant, $U = U(x)$, u, v are small disturbance quantities.

Linearising the Navier Stokes equations with respect to u and v, we get

$$U U_x + u U_x + U u_x + v U_y = -\frac{1}{\rho} p_x + \nu \nabla^2 u \qquad (2)$$

$$U v_x = -\frac{1}{\rho} p_y + \nu \nabla^2 v - g \qquad (3)$$

Combining the equation vectorially, we can write

$$U \vec{q}_x + U U_x + u U_x + v U_y = -\frac{1}{\rho} \nabla (p + \rho g y^{(4)}) + \nu \nabla^2 \vec{q}$$

Let us assume that

$$\vec{q} = \vec{q}_1 + \vec{q}_2$$

such that $\text{Curl}\ \vec{q}_1 = 0$ and $\text{div}\ \vec{q}_2 = 0$ (5)

i.e. $\vec{q}_1$ is potential and $\vec{q}_2$ is solenoidal.

Substituting (5) into (4) we get

$$U(\vec{q}_{1x} + \vec{q}_{2x}) + (U+u)U_x + vU_y = \nabla(p/\rho + gy) + \nu\nabla^2\vec{q} \quad (6)$$

Taking curl on both sides, we obtain

$$\text{curl}\{U(\vec{q}_{1x} + \vec{q}_{2x})\} + \text{curl}\{(U+u)U_x + vU_y\} = \nu\nabla^2\,\text{curl}(\vec{q}_1 + \vec{q}_2) \quad (7)$$

Now, if U = constant, we would get

$$U\vec{q}_{2x} = \nu\nabla^2\vec{q}_2 \quad (8)$$

which is an equation only in $\vec{q}_2$.

But this is not possible if U is not a constant. Once again, taking divergence of the equation (4), we get

$$\operatorname{div}\{U(\vec{q}_{1x}+\vec{q}_{2x})\} + \operatorname{div}\{(U+u)U_x + v U_y\}$$

$$= -\operatorname{div}\nabla(p/\rho + gy) + \nu\nabla^2 \operatorname{div}(\vec{q}_1+\vec{q}_2)$$

If U = constant, we would get

$$U\vec{q}_{1x} = -\nabla(p/\rho + gy) + \nu\nabla^2\vec{q}_1$$

which is an equation only in q_1 .

Hence we find that the flow is not separable into potential and solenoidal components if U is not constant. Consequently the technique of Wu and Messick (1958) can no longer be applied in this case.

APPENDIX B

The general solution of equation (2.68) should correspond to

$$P_1 U a' + (2P_1 + 2P_2 + 3) a U' = 0$$

This can be written as

$$\frac{a'}{a} + K_2 \frac{U'}{U} = 0$$

where $$K_2 = \frac{2P_1 + 2P_2 + 3}{P_1}$$

The integration of the above equation gives

$$a = \frac{K_3}{U^{K_2}}$$

where K_3 is a constant of integration.

Since a should vanish at $x = -\infty$ where $U = U_\infty$, so K_3 should be equal to zero. Hence

$$a = 0$$

is the general solution of the equation.

REFERENCES

Baba, E., A New Component of Viscous Resistance of Ships, Journal of Society of Naval Architects of Japan, Vol. 125 (1969), pp 23-34.

Batchelor, G.K., An Introduction to Fluid Mechanics, Cambridge Univ. Press (1970).

Baba, E., Some Free Surface Phenomena around Ship to be Challenged by Numerical Analysis, 3rd Internat. Conf. on Numerical Ship Hydrodynamics, Paris (1981).

Cumberbatch, E., Effects of Viscosity on Ship Waves, J. Fluid Mech., Vol. 23 (1965), pp 471-479.

Dagan, G. and Tulin, M.P., Two-Dimensional Free Surface Gravity Flow Past Blunt Bodies, J. Fluid Mech., Vol. 51 (1972), pp 529-543.

Dagan, G. and Tulin, M.P., Taylor Instability of a Non-Uniform Free Surface Flow, J. Fluid Mech., Vol. 67 (1975), pp 113-123.

Eckert, E. and Sharma, S.D., Bugwülste fur langsame, völlige Schiffe, Jahrb. Schiffbautech. Ges. 64 (1970), pp 129-171.

Hawthorne, W.R., Secondary Flow about Struts and Airfoils, J. Aeronautical Soc., Vol. 21 (1954), pp 588-608.

Harper, J.F. and Dixon, J.N., The Leading Edge of a Surface Film on Contaminated Flowing Water, Proc. 5th Australian Conf. on Hydraulics and Fluid Mechanics (1974), pp 499-505.

Honji, H., Observation of a Vortex in Front of a Half-Submerged Circular Cylinder, J. Physical Society of Japan, Vol. 40, No. 5 (1976).

Kayo, Y. and Takekuma, K., On the Free Surface Shear Flow Related Bow Wave Breaking of Full Ship Models, J. Soc. Naval Arch., Japan, Vol. 149 (1981), pp 11-20.

Kayo, Y., Takekuma, K., Eggers, K. and Sharma, S.D., Observation of Free Surface Shear Flow and its Relation to Bow Wave Breaking on Full Forms, Inst. Schiffban, Univ. Hamburg, Report 420 (1982).

Kayo, Y. and Takekuma, K., Shear Layer and Secondary Vortical Flow beneath Free Surface around Bow of Full-Form Ship Model, Trans., West Japan Soc. Naval Arch., No. 65 (1983).

Lamb, H., Hydrodynamics, Cambridge Univ. Press (1932).

Lighthill, M.J., Drift, J. Fluid Mech., Vol. 1 (1956), pp 31-53.

Miyata, H., Kajitani, H., Suzuki, N. and Matsukawa, C., Numerical and Experimental Analysis of Non-Linear Bow and Stern Waves of a Two-Dimensional Body, J. of Society of Naval Architects of Japan, Vol. 154 (1983).

Miyata, H. et al., Numerical and Experimental Analysis of Non-Linear Bow and Stern Waves of a Two-Dimensional Body (Second and Third Reports respectively), Spring Meeting of SNAJ, May (1984a) and Autumn Meeting, Nov. (1984b).

Miyata, H. and Inui, T., Non-Linear Ship Waves, Advances in Applied Mechanics, Vol. 24 (1984).

Mori, K.H., Necklace Vortex and Bow Wave around Blunt Bodies, 15th ONR Symposium on Naval Hydrodynamics, 2-7 Sept. (1984), Hamburg.

Miyata, H. and Nishimura, S., Finite Difference Simulation of Non-Linear Ship Waves, J. Fluid Mech., Vol. 157 (1985), pp 327-357.

Maruo, H. and Ikehata, M., Some Discussions on the Free Surface Flow around the Bow, 16th Symposium on Naval Hydrodynamics, July (1986).

Ogiwara, S., Masuko, A., Sato, R. and Tsutsumi, T., Experimental Investigation on Free Surface Flow Related to Bow Wave Breaking, Journal Kansai SNAJ, Vol. 194, Sept. (1984), pp 119-132.

Patel, V.C., Landweber, L. and Tang, C.J., Free Surface Boundary Layer and the Origin of Bow Vortices, Second Internat. Symp. on Viscous Resistance (1985), Goteborg, Sweden.

Shahshahan, A., Study of Free-Surface Flow near a Ship Bow, The University of Iowa, Iowa, Master's Thesis, July (1981).

Scott, J.C., Flow beneath a Stagnant Film on Water: the Reynolds Ridge, J. Fluid Mech., Vol. 116 (1982), pp 283-296.

Suzuki, K., On the Drag of Two-Dimensional Bluff Bodies Semi submerged in Surface Flow, Journ.Soc. Naval Architects Japan (in Japanese), Vol. 137 (1975), pp. 22-35.

Taneda, S. and Amamoto, H., On the Necklace Vortex, Bulletin of Res. Inst. Appl. Mech., Kyushu Univ., No. 31, Japanese (1969).

Taniguchi, K., Tamura, K. and Baba, E., Reduction of Wave-Breaking Resistance 'MHI-Bow' Mitsubishi Juko Giho Vol. 8, No. 1 (1971), pp 146-152, Japanese or Mitsubishi Technical Review, Vol. 9, No. 1 (1972), pp 62-69, English.

Takekuma, K., Study on the Non-Linear Free Surface Problem around bow, J. Soc. Naval Arch. Japan, Vol. 132 (1972), pp 1-9.

Takekuma, K. and Eggers, K., Effect of Bow Shapes on the Free Surface Shear Flow, Proc. 15th ONR Symposium on Naval Hydrodynamics, 2-7 Sept. (1984), Hamburg, pp. 387-405.

Tuck, E.O. and Vanden-Broeck, J. M. , Splashless Bow Flows in Two-Dimensions , 15th Symposium on Naval Hydrodynamics, Hamburg Sept. (1984).

Wu, T.Y. and Messick, R.E., Viscous Effects on Surface Waves Generated by Steady Disturbances, California Inst. of Technology, Engineering Division, Report No. 85-8 (1958).

LIST OF SYMBOLS

s, n - curvilinear coordinates, Fig. 4

u, v - velocity components corresponding to the coordinate system

k - curvature of the free surface

ρ - density

g - acceleration due to gravity

ν - kinematic viscosity

p - fluid pressure

p_a - atmospheric pressure

x, y - Cartesian coordinate system

μ - coefficient of viscosity

r - radius of the cylinder

L - reference length (= $2r$)

U_∞ - velocity at ∞

F - Froude number (= $U_\infty / \sqrt{g \cdot 2r}$)

R_e - Reynolds number (= $U_\infty \cdot 2r / \nu$)

W - Weber number (= $\rho U_\infty^2 \cdot 2r / \sigma$)

U_1, V_1 - potential flow velocity components corresponding to x, y coordinate system

U, V - potential flow velocity components corresponding to s, n coordinate system

δ - boundary layer thickness

δ_1 - displacement thickness

u_D - velocity difference variable (= $u - U$)

σ - surface tension

k_1, k_2 - wave numbers of gravity waves in presence of surface tension

ζ - free surface elevation

$(')$ - derivative with respect to S.

Table 1 Numerical values of nondimensional displacement thickness (δ_1), shape factors (P_1 & P_2), velocity defect (a) and the free surface curvature k at various positions (x) for a cylinder of radius .05 m .

F = .252 R_e = 20450.82

x	δ_1	P_1	P_2	a	k
-10.0	0.5027×10^{-7}	-0.2283	0.1124×10^{-4}	-0.4418×10^{-5}	0.7520×10^{-4}
-9.0	0.7051×10^{-7}	-0.2545	0.1538×10^{-4}	-0.6173×10^{-5}	0.1142×10^{-3}
-8.0	0.1025×10^{-6}	-0.2864	0.2177×10^{-4}	-0.8972×10^{-5}	0.1818×10^{-3}
-7.0	0.1564×10^{-6}	-0.3267	0.3221×10^{-4}	-0.1373×10^{-4}	0.3077×10^{-3}
-6.0	0.2542×10^{-6}	-0.3793	0.5037×10^{-4}	-0.2247×10^{-4}	0.5628×10^{-3}
-5.0	0.4517×10^{-6}	-0.4601	0.8982×10^{-4}	-0.4318×10^{-4}	0.1235×10^{-2}
-4.0	0.9174×10^{-6}	-0.5569	0.1580×10^{-3}	-0.8375×10^{-4}	0.2676×10^{-2}
-3.0	0.2322×10^{-5}	-0.7280	0.3373×10^{-3}	-0.2183×10^{-3}	0.7693×10^{-2}
-2.0	0.9147×10^{-5}	-1.0573	0.8012×10^{-3}	-0.9032×10^{-3}	0.2786×10^{-1} ,

Contd...

Table 1 (Contd.)

x	δ_1	P_1	P_2	a	k
-1.5	0.2721×10^{-4}	-1.3558	0.8263×10^{-3}	-0.2849×10^{-2}	0.3906×10^{-1}
-1.4	0.3661×10^{-4}	-1.4268	0.5812×10^{-3}	-0.3940×10^{-2}	0.2970×10^{-1}
-1.3	0.5183×10^{-4}	-1.4944	0.6601×10^{-4}	-0.5857×10^{-2}	0.3684×10^{-2}
-1.2	0.1608×10^{-3}	-1.4787	0.9150×10^{-3}	-0.2062×10^{-1}	-0.5788×10^{-1}
-1.15	0.2820×10^{-3}	-1.4799	0.1684×10^{-2}	-0.3870×10^{-1}	-0.1135
-1.10	0.6272×10^{-3}	-1.4877	0.2739×10^{-2}	-0.9125×10^{-1}	-0.1968
-1.05	0.2281×10^{-2}	-1.4982	0.4191×10^{-2}	-0.3517	-0.3217
-1.04	0.3301×10^{-2}	-1.5002	0.4541×10^{-2}	-0.5271	-0.3535
-1.03	0.5135×10^{-2}	-1.5019	0.4914×10^{-2}	-0.8243	-0.3879
-1.02	0.8755×10^{-2}	-1.5034	0.5312×10^{-2}	-1.4141	-0.4253
-1.01	0.1731×10^{-1}	-1.5047	0.5735×10^{-2}	-2.8626	-0.4658

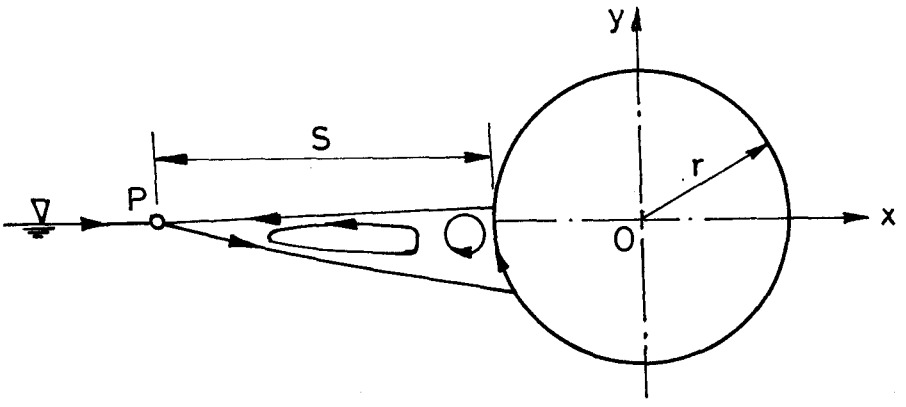

FIG.1. VORTICES AHEAD OF A HORIZONTAL CYLINDER

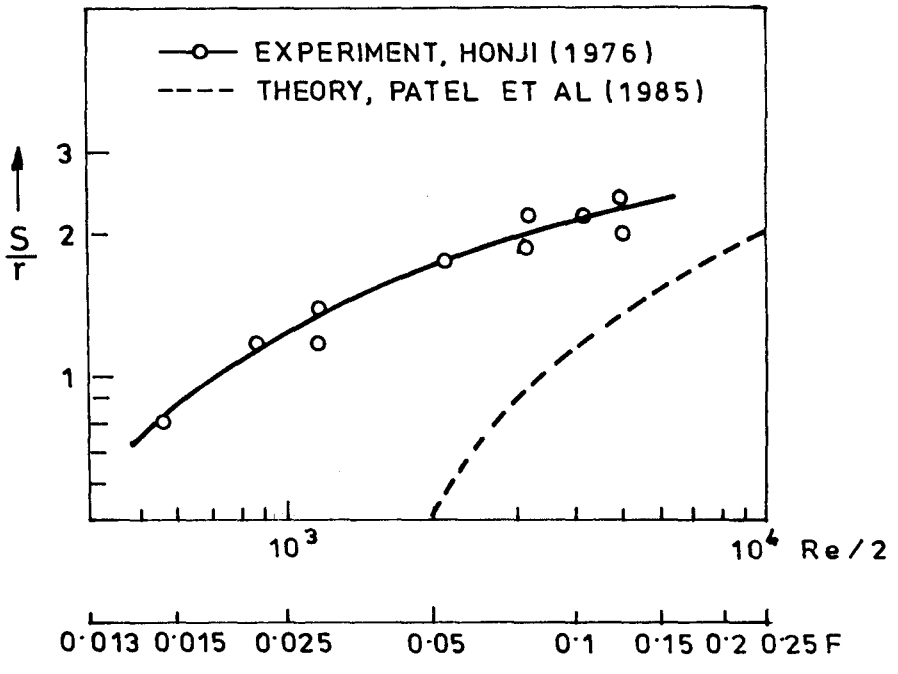

FIG.2. SEPARATION CRITERION FOR A HORIZONTAL CIRCULAR CYLINDER

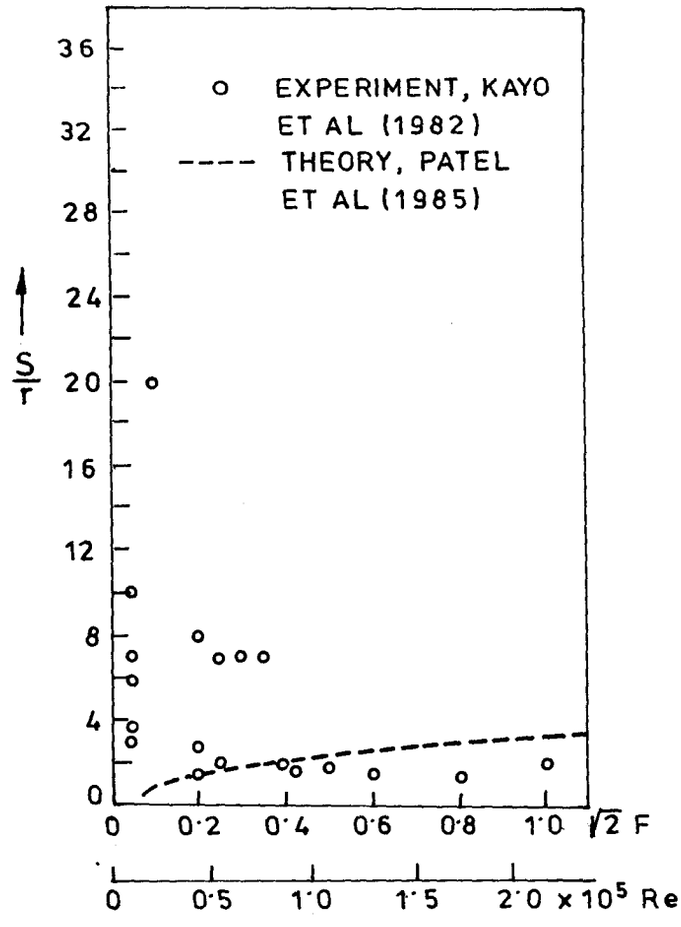

FIG. 3. SEPARATION CRITERION FOR A HORIZONTAL CIRCULAR CYLINDER

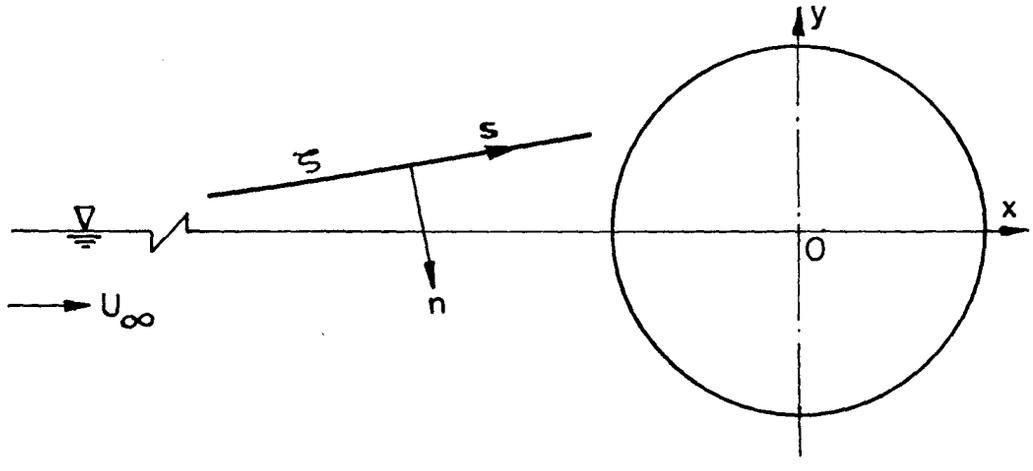

FIG. 4. CO-ORDINATE SYSTEM

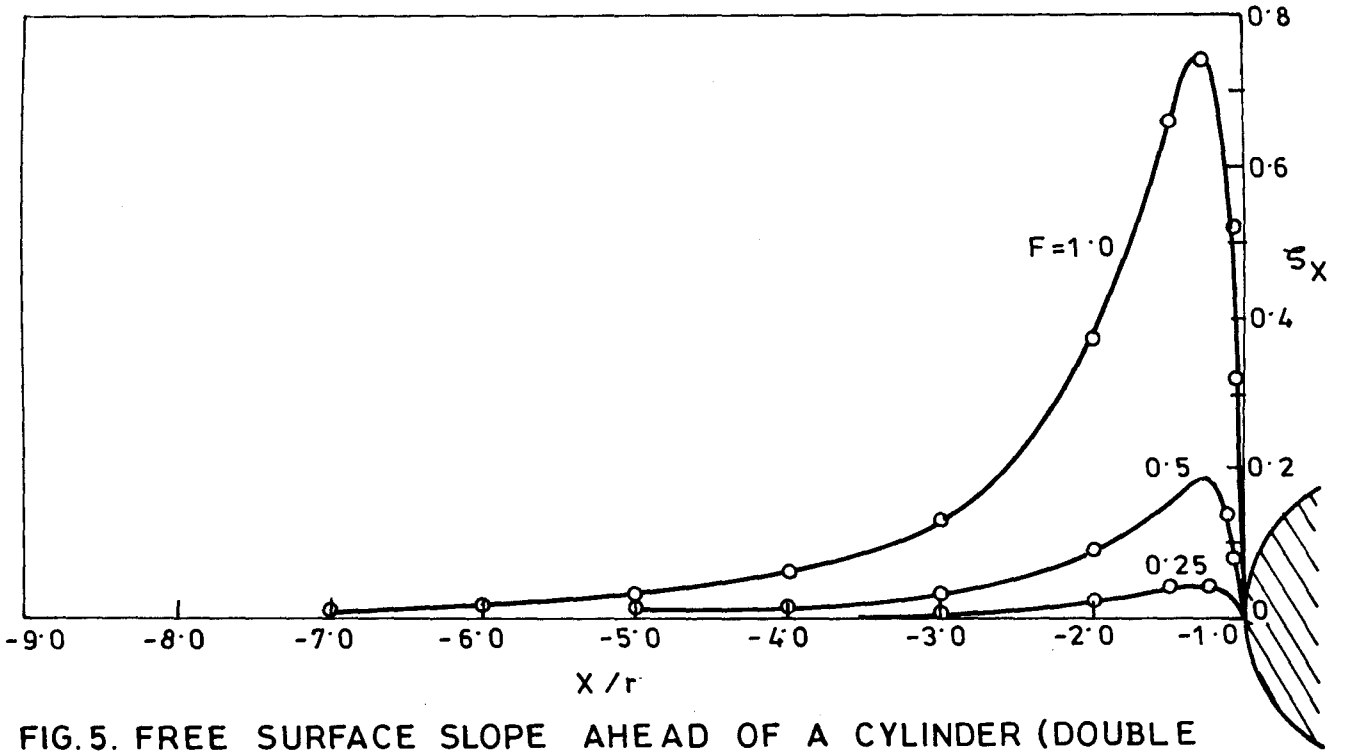

FIG. 5. FREE SURFACE SLOPE AHEAD OF A CYLINDER (DOUBLE BODY APPROXIMATION)

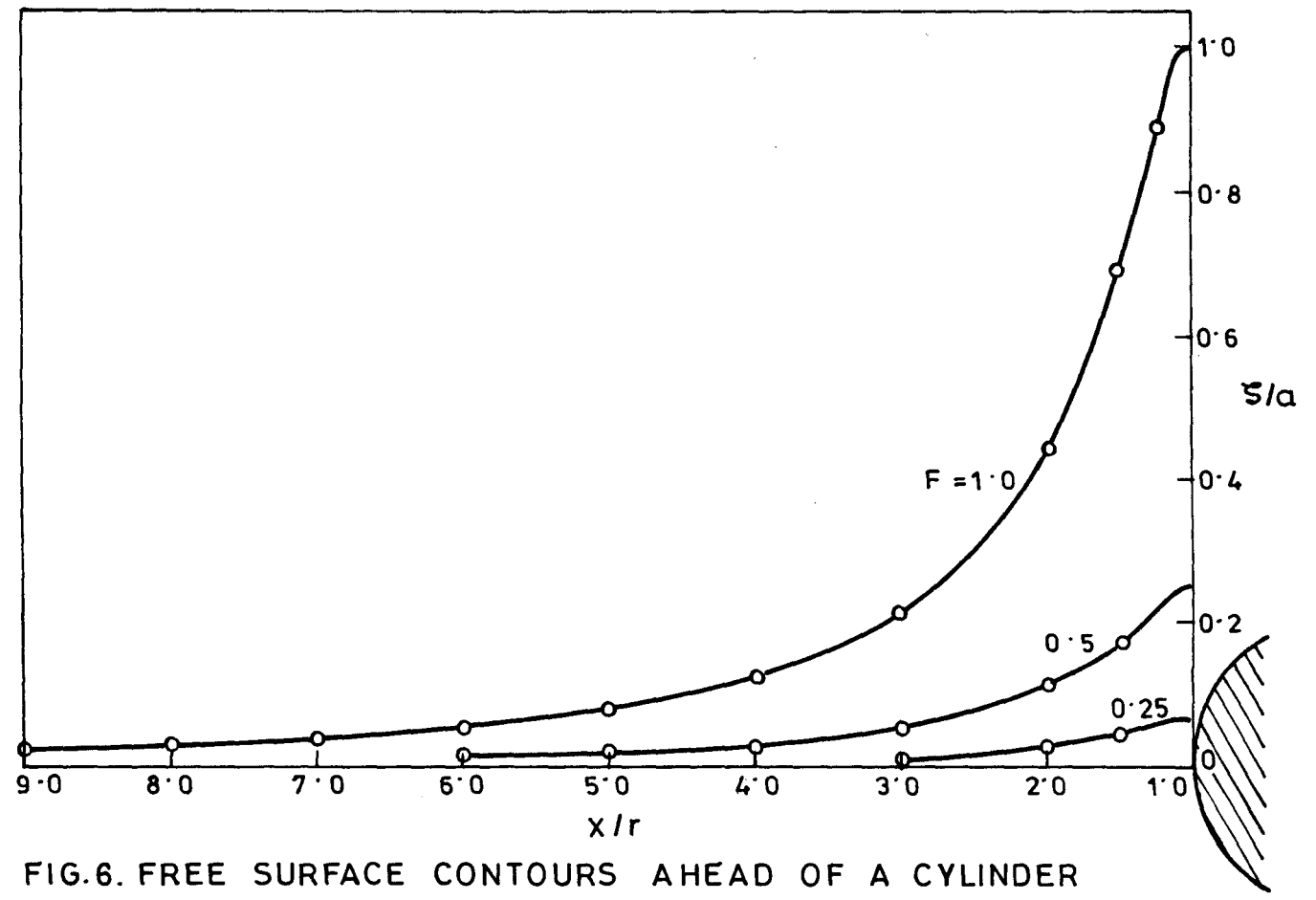

FIG. 6. FREE SURFACE CONTOURS AHEAD OF A CYLINDER (DOUBLE BODY APPROXIMATION)

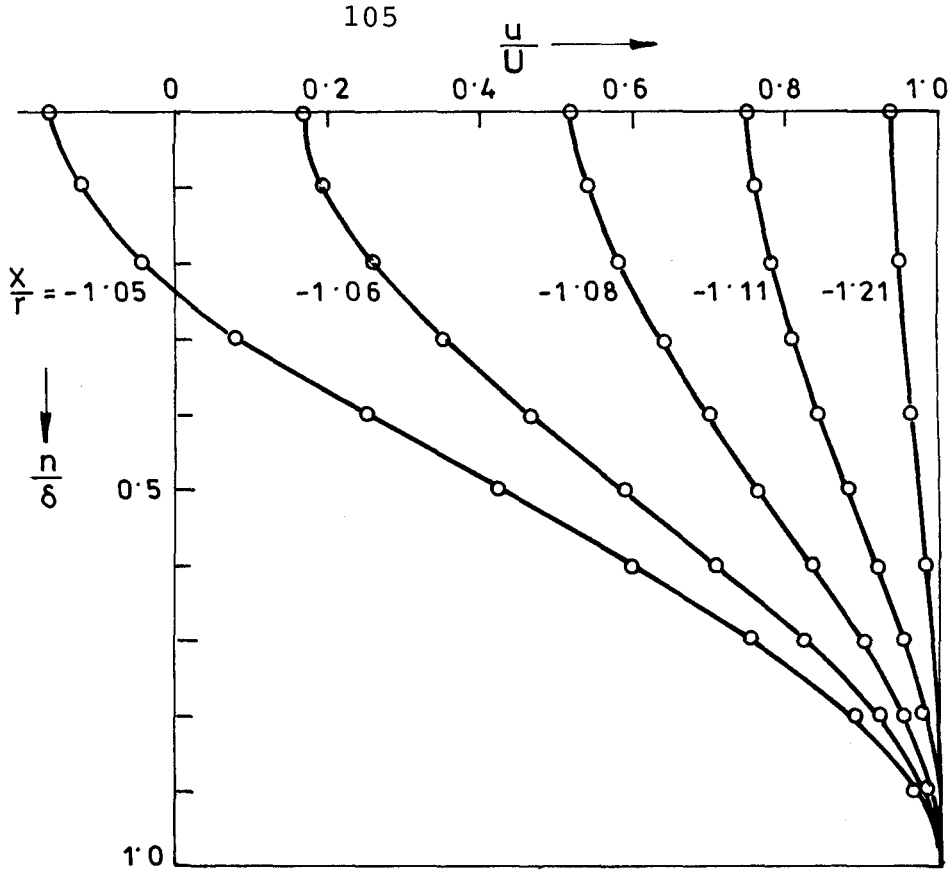

FIG. 7. FREE SURFACE SHEAR LAYER VELOCITY PROFILES, F = 0·5

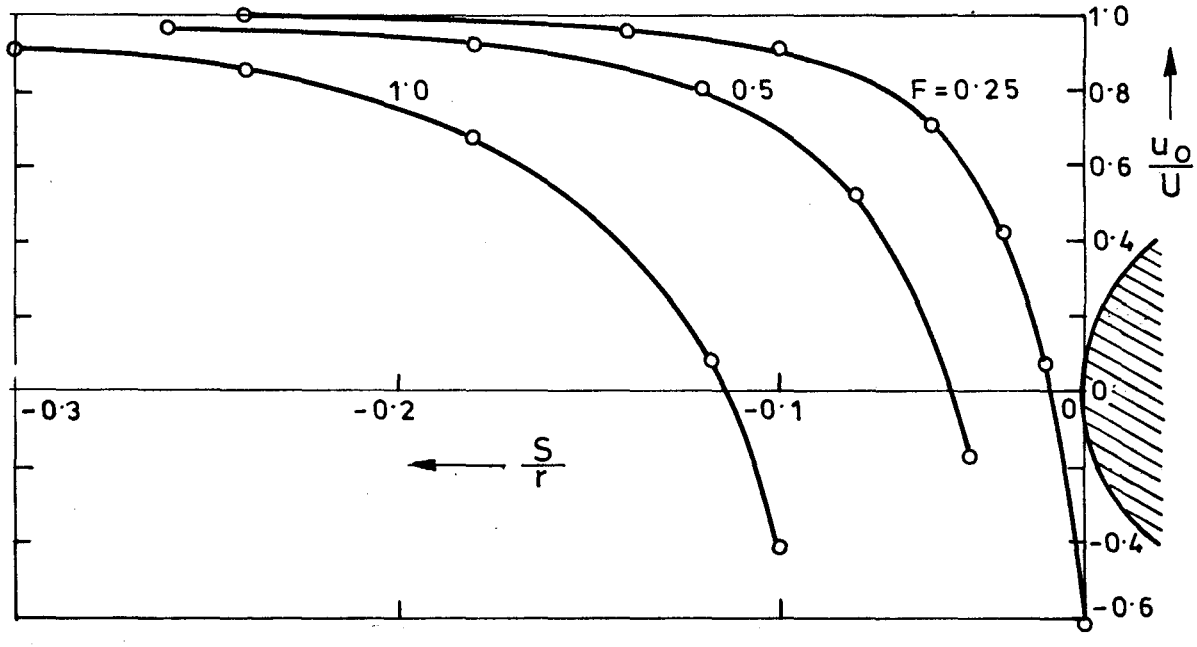

FIG. 8. SHIFT IN THE POSITION OF THE FREE SURFACE SEPARATION POINT WITH FROUDE NUMBER

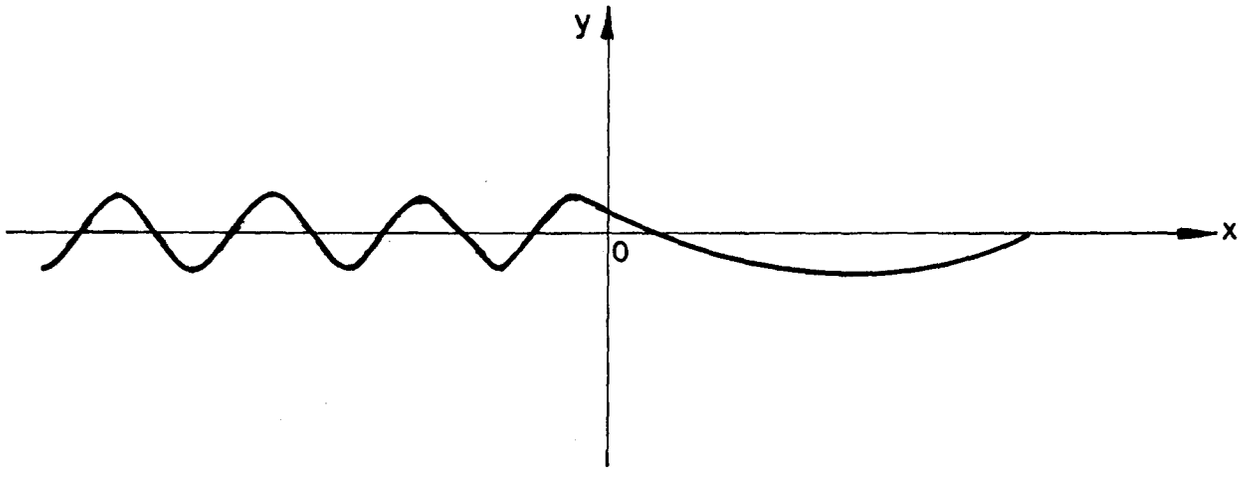

FIG. 9. GRAVITY AND CAPILLARY WAVE SYSTEM DUE TO A CONCENTRATED PRESSURE AT THE ORIGIN

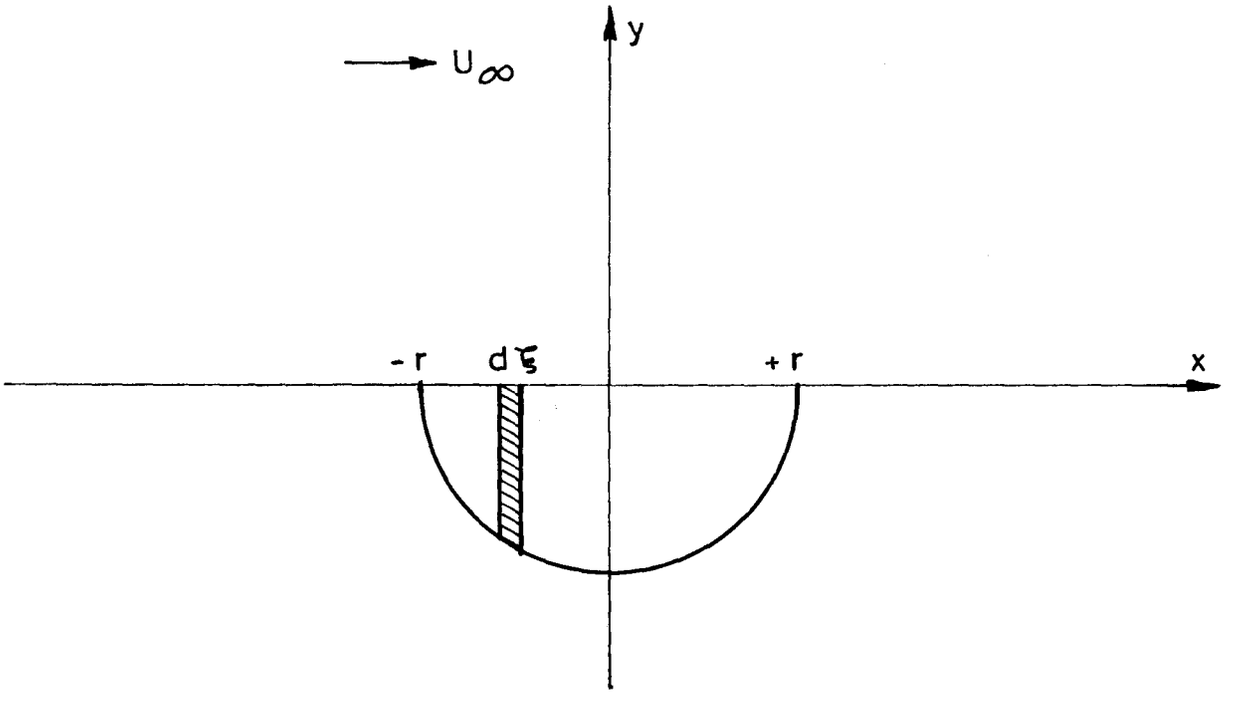

FIG. 10. FLAT SHIP APPROXIMATION FOR PRESSURE DISTRIBUTION.